ALMA MATER STUDIORUM
UNIVERSITÀ DI BOLOGNA

DEPARTMENT OF DEPARTMENT OF PHYSICS AND ASTRONOMY "A. RIGHI"

SECOND CYCLE DEGREE

APPLIED PHYSICS

OPTIMIZATION OF LET DISTRIBUTION IN PROTON BEAM THERAPY FOR BRAIN TUMORS

Supervisor

Roberto Spighi

Co-Supervisor

Alessandro Vai

Silvia Molinelli

Defended by

Valeriia Tolstoukhova

Graduation Session 24-25 July 2025

Academic Year 2024/2025

Abstract

This thesis explores the potential clinical impact of integrating LET (Linear Energy Transfer) optimization into the treatment planning workflow for proton therapy of brain tumors. Recent advances in treatment planning systems (TPS) have introduced the ability not only to visualize LET distributions, but also to directly incorporate LET optimization into the planning process. Despite growing recognition of the biological importance of LET in the literature, a broad consensus on clinical reference values (e.g., LET thresholds at specific dose levels) to guide decision-making in brain tumor cases is still lacking.

In the first phase of this study, a normal tissue complication probability (NTCP) model was developed based on LETd values derived from a retrospective clinical cohort of brain tumor patients treated and followed up at CNAO. Subsequently, a group of 20 patients with similar morphological and dosimetric characteristics was selected for further analysis. Each patient had an approved clinical treatment plan, which served as a baseline for multiple rounds of re-optimization using various LET-oriented strategies.

LET optimization was studied both for the currently used fixed-beam geometry available at CNAO and for a gantry-based beam arrangement (360° around the transverse plane of the patient), in anticipation of the future installation of a gantry system at CNAO. These strategies aimed to reduce LETd in healthy brain structures while maintaining clinically acceptable dose distributions. Optimization was performed for both geometries, and the resulting plans were comprehensively analyzed across three critical dimensions: (1) dose distribution quality—i.e., an acceptable compromise between therapeutic high dose to the target and tolerable dose to surrounding healthy tissue; (2) LETd maps; and (3) robustness against clinically relevant uncertainties. This approach enabled the identification of optimal trade-offs between these competing aspects within a realistic clinical workflow.

Importantly, the impact of LETd reduction achieved through this optimization workflow was quantitatively translated into a lower predicted risk of radiation-induced side effects, based on the previously developed NTCP model. The findings showed that LETd-optimized plans—particularly gantry-based plans with stronger LET constraints—achieved reductions in LETd of up to 5.6% in the brain, without compromising target coverage, robustness, or tumor LET distribution.

These results confirm both the feasibility and clinical relevance of incorporating LET-based constraints into proton therapy planning. The proposed strategies may serve as practical guidelines to enhance treatment safety and biological effectiveness for patients with brain tumors.

Keywords: *Proton Therapy, LET Optimization, Radiation-Induced Healthy Tissue Toxicity, Proton Plan Robustness, Normal Tissue Complication Probability*

Acknowledgements

I would like to express my sincere gratitude to all those who supported me and contributed to the completion of this thesis.

First and foremost, I am deeply thankful to my research supervisor, Alessandro Vai, for his invaluable guidance, attentiveness, patience, and continuous support throughout this project. His insightful advice and recommendations not only helped me gain a deeper understanding of the topic, but also significantly enriched my professional development.

My special thanks go to Silvia Molinelli for her thoughtful feedback, willingness to share her expertise, and assistance during the research process.

I am also grateful to CNAO (National Center for Oncological Hadrontherapy) for providing access to advanced equipment and resources, without which this study would not have been possible. I extend my heartfelt thanks to the entire medical physics team for their warm welcome, practical assistance, and essential guidance, which enabled me to engage with the complex and inspiring field of hadron therapy.

I wish to express my appreciation to my academic supervisor, Professor Roberto Spighi, for introducing me to the field of hadron therapy, and for his support, thoughtful advice, and recommendations that helped me improve the quality of my work.

Finally, I would like to thank my family for their unconditional love, encouragement, and belief in me — even when it meant letting me go halfway across the world in pursuit of a dream. I am especially grateful to my parents for always nurturing my curiosity and passion for science, and for showing me, by their own example, how to work hard and find joy in the process. I am also grateful to my friends for their warmth, patience, and understanding, especially during the most intense periods of writing and concentration.

Table of Contents

List of Figures

List of Tables

List of Acronyms and Abbreviations

- **LET** – *Linear Energy Transfer*
  The amount of energy deposited by ionizing radiation per unit length of tissue traversed, typically expressed in keV/μm.
- **LETd** – *Dose-Averaged Linear Energy Transfer*
  A weighted average of LET values, considering the dose contribution from each energy deposition event; used to quantify the biological impact of proton therapy.
- **DNA** – *Deoxyribonucleic Acid*
  The molecule that carries genetic information in living organisms and is a primary target for radiation-induced cellular damage.
- **PBS** – *Pencil Beam Scanning*
  A proton delivery technique in which narrow proton beams are magnetically steered to deliver dose precisely to the target in a spot-by-spot and layer-by-layer manner.
- **IMPT** – *Intensity-Modulated Proton Therapy*
  An advanced form of PBS in which both intensity and position of proton spots are optimized to achieve highly conformal dose distributions.
- **PMAT** – *Pencil Beam Modulated Arc Therapy*
  A technique combining pencil beam scanning with arc-based delivery, allowing for continuous gantry rotation and dynamic modulation of beam parameters.
- **RBE** – *Relative Biological Effectiveness*
  A factor used to compare the biological effectiveness of different types of radiation, defined as the ratio of doses required by reference radiation and the tested radiation to produce the same biological effect.
- **VMAT** – *Volumetric Modulated Arc Therapy*
  An advanced photon-based radiation therapy technique that delivers dose by rotating the gantry around the patient while modulating the beam intensity, shape, and dose rate.
- **OARs** – *Organs at Risk*
  Normal tissues or critical structures that are sensitive to radiation and must be protected during treatment planning to minimize side effects.
- **DVH** – *Dose–Volume Histogram*
  A graphical representation showing the percentage or absolute volume of a structure receiving at least a given dose, used to evaluate the quality of a treatment plan.
- **PTV** – *Planning Target Volume*
  A volume that includes the clinical target volume (CTV) plus margins to account for setup uncertainties and patient movement, ensuring the prescribed dose is delivered effectively, in accordance with ICRU Report 83.
- **CTV** – *Clinical Target Volume*
  The tissue volume that contains a demonstrable tumor and/or subclinical malignant disease that needs to be eliminated, in accordance with ICRU Report 83.
- **GTV** – *Gross Tumor Volume*
  The visible or clinically detectable extent and location of the malignant growth, in accordance with ICRU Report 83.
- **SRT** – *Stereotactic Radiotherapy*
  A highly precise form of radiation therapy that delivers high doses to small targets with millimeter accuracy.

- **SOBP** – *Spread-Out Bragg Peak*
  A proton beam modification technique that combines multiple Bragg peaks to create a uniform dose distribution across the tumor depth.
- **LDVH** – *LET–Dose Volume Histogram*
  A histogram combining LET and dose data to illustrate the relationship between energy deposition and volume, aiding in the assessment of biological effectiveness during treatment planning.
- **MaxLETd** – *Maximum Dose-Averaged LET*
  An optimization function used to constrain the maximum dose-averaged LET within a specified structure. It is primarily applied to reduce the biological impact on critical organs located near the target volume.
- **MaxLVH** – *Maximum LET–Volume Histogram Value*
  An LET-based optimization function designed to limit the volume of tissue receiving LET above a defined threshold, as derived from the LET–volume histogram (LVH). It allows for more precise control of high-LET regions, particularly in radiosensitive areas.
- **CT** – *Computed Tomography*
  A medical imaging technique used to generate detailed cross-sectional images of the body, commonly used for treatment planning in radiotherapy.
- **NTCP** – *Normal Tissue Complication Probability*
  A predictive model estimating the probability of radiation-induced complications in healthy tissues based on dose-volume parameters.
- **TPS** – *Treatment Planning System*
  Specialized software used in radiotherapy to design, optimize, and evaluate radiation treatment plans.
- **HI** – *Homogeneity Index*
  A metric used to quantify the uniformity of the dose distribution within the target volume.
- **CI** – *Conformity Index*
  A measure of how well the radiation dose conforms to the shape of the target volume.
- **D95%** – *Dose to 95% of the Volume*
  The minimum dose received by 95% of the target volume, commonly used to assess target coverage.
- **D98%** – *Dose to 98% of the Volume*
  The dose covering 98% of the volume, used to evaluate near-minimum dose delivered to the target.
- **D1%** – *Dose to 1% of the Volume*
  The dose received by the hottest 1% of the volume, often used to assess hot spots.
- **D1cc** – *Dose to 1 Cubic Centimeter*
  The highest dose received by any 1 cm^3 of a structure, typically used for organs at risk.

Introduction

1. Proton vs Photon-Based Radiation Treatments in Clinical Practice: Advantages and Limitations

Radiation therapy is one of the most widely used cancer treatment modalities, applied in more than half of all oncology cases — either as a standalone intervention or in combination with surgery, chemotherapy, or immunotherapy [1], [2]. It is based on the use of ionizing radiation to damage the DNA of malignant cells, potentially leading to cell death or loss of reproductive capacity. Among the available radiation modalities, proton therapy is gaining prominence due to its unique physical property known as the Bragg peak — where the majority of the proton's energy is deposited at a specific depth in tissue, with almost no exit dose beyond the target [3]. This allows for better sparing of healthy tissues and critical structures, especially in the treatment of tumors located in sensitive anatomical regions such as the brain [4], [5], [6], [7].

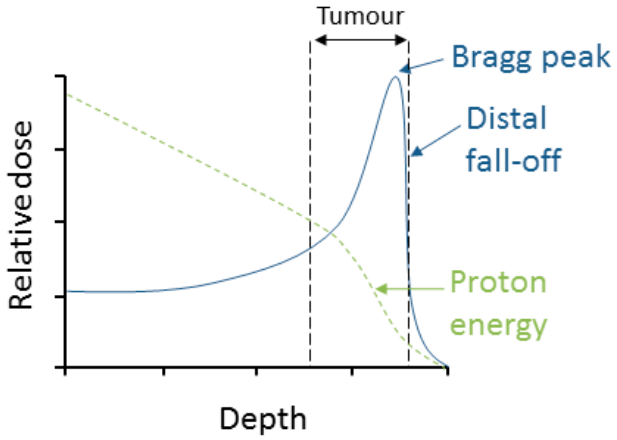

Figure 1. *Depth–dose distribution of protons and relationship to energy and linear energy transfer (LET). Reproduced from Vitti E.* Cancers (2019), 11(7), 946, *[7]*

The theoretical foundation of proton therapy dates back to 1946, when Robert R. Wilson first proposed its clinical application. Practical use began in the 1950s. However, its widespread integration into clinical practice became feasible only in the late 20th and early 21st centuries, owing to advancements in accelerator technology and imaging techniques [4]. Today, proton therapy is among the most rapidly developing forms of external beam radiation therapy and is being actively implemented worldwide [PTCOG website, accessed March 2025]. Since the early 2020s, the number of specialized centers has been steadily increasing: more than 120

facilities are currently operational in the United States, Europe, and Asia, with many others under construction or in the planning phase reflecting the global expansion of this advanced radiation modality.

Building upon these advancements and growing clinical implementation, modern proton therapy is primarily delivered using intensity-modulated proton therapy (IMPT) and pencil beam scanning (PBS) techniques. This approach enables the creation of highly conformal treatment plans with precise control over dose distribution in three-dimensional space [8]. This approach enables the creation of highly conformal treatment plans with precise control over dose distribution in three-dimensional space. Unlike photon therapy, where gantry systems are standard and fully integrated into all linear accelerators, gantry systems in proton therapy are technically more complex and significantly increase installation and operational costs. Many proton centers utilize fixed beamlines (horizontal or vertical), which limit beam angle selection and may lead to increased dose exposure to healthy tissues—especially when treating tumors located near critical structures. The use of gantry systems in proton therapy allows for rotational beam delivery, expanding the range of possible angles and thereby enhancing planning flexibility. Modern techniques such as proton monoenergetic arc therapy (PMAT) [9] and advanced beam orientation optimization algorithms [10] have demonstrated that gantry use can improve target coverage while simultaneously reducing the biological burden on surrounding healthy tissue. In parallel, there is ongoing development and implementation of novel treatment planning strategies in proton therapy, such as robust optimization [11], linear energy transfer (LET)-based optimization [12], and variable relative biological effectiveness (RBE) modeling [3], all aimed at improving the precision, predictability, and safety of treatment.

A representative clinical application of the advantages of proton therapy is in the treatment of brain tumors, where the physical properties of protons enable highly selective dose distributions in scenarios that demand maximum precision.

1.1. Modern Approaches to Brain Tumor Treatment: Stereotactic Radiotherapy and Proton Therapy

Although photon-based radiation therapy remains a cornerstone of modern cancer treatment due to its wide availability and well-established clinical protocols, proton therapy offers distinct physical advantages—particularly in the stereotactic treatment of brain tumors, a technique based on the highly precise delivery of radiation to a defined target in three-dimensional space. Photon-based stereotactic radiotherapy techniques, such as volumetric modulated arc therapy (VMAT) or multi-beam intensity-modulated radiation therapy (IMRT), provide high spatial accuracy but inevitably result in broader low-dose exposure to surrounding normal tissues, especially in deeply located lesions or those adjacent to critical structures.

In contrast to photon therapy, proton therapy takes advantage of the Bragg peak to deliver highly conformal doses with a sharp distal fall-off, resulting in reduced integral dose to healthy tissues. This physical advantage is particularly beneficial in stereotactic treatments of brain tumors, where precise targeting and maximal tissue sparing are critical.

This advantage is particularly evident in the treatment of intracranial tumors such as meningiomas, vestibular schwannomas, or craniopharyngiomas, which are often situated near sensitive structures including the brainstem, optic chiasm, and temporal lobes. The difference in dose distribution between photon and proton stereotactic radiotherapy is illustrated by a representative case of craniopharyngioma treatment (***Figure 2***) [13].

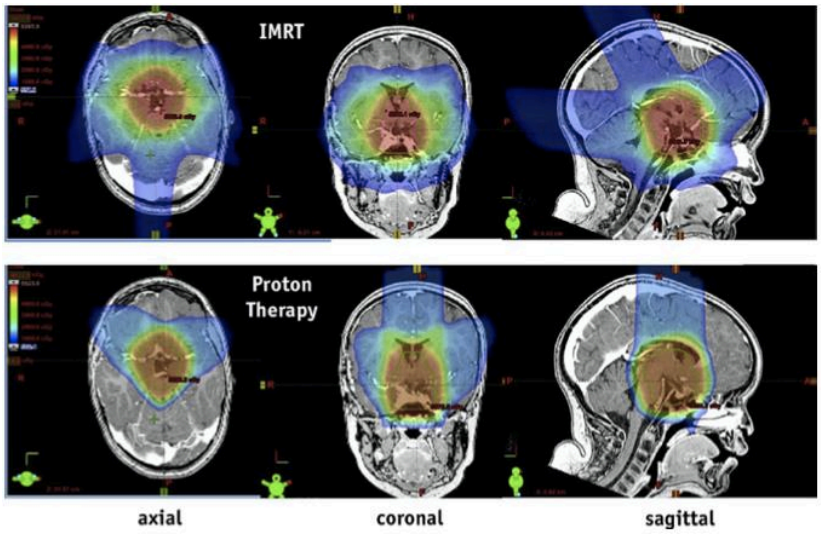

Figure 2. *Comparison of dose distributions in the treatment of craniopharyngioma: photon therapy (IMRT, top row) and proton therapy (bottom row) in axial, coronal, and sagittal*

planes. Reproduced from: Indelicato DJ et al. Int J Radiat Oncol Biol Phys. 2016;96(2):387–392. [13]

Dosimetric comparisons between stereotactic photon and proton therapy plans demonstrate that proton therapy consistently provides comparable or improved target coverage, while significantly reducing the dose to surrounding organs at risk (OARs). A concise and widely used method to represent dose distribution within a treatment plan is the dose-volume histogram (DVH).

The DVH is a graphical representation that shows the percentage volume of a given structure receiving at least a specified dose. It offers essential information regarding the dose distribution across both the planning target volume (PTV) and the OARs. In an ideal treatment plan, where 100% of the prescribed dose is delivered uniformly to the entire PTV and no dose is delivered to any OAR, the DVH for the PTV appears as the positive half of a top-hat function, while the DVH for the OAR remains at zero across all dose values. In clinical practice, however, such perfect dose conformity is rarely achievable. Dose fall-off near the PTV often results in underdosed (cold spots) or overdosed (hot spots) regions [14]. These deviations are reflected in the DVH by inward or outward bending of the curve, as illustrated in curve 3. Additionally, when an OAR is located adjacent to the PTV, some dose spillover is inevitable, which is represented by curve 4 in ***Figure 3***. The amount of radiation dose considered clinically acceptable is based on international guidelines, which are grounded in radiobiological principles and supported by dose-escalation studies [15]. In our study, we specifically analyze the brain and brainstem, which share a boundary with the target volume; as a result, the maximum dose delivered to these structures—albeit limited to a small volume—can approach or even coincide with the prescribed dose.

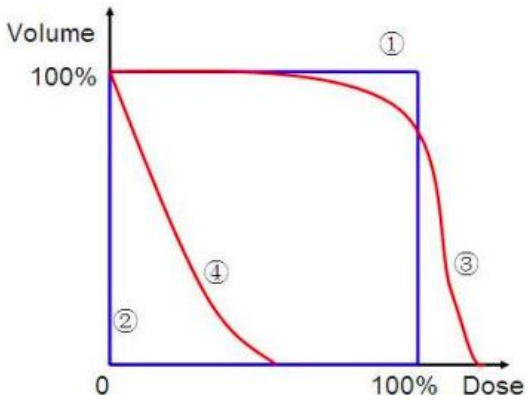

Figure 3. *Ideal PTV and OAR DVH curves (1 - 2) and typical real PTV and OAR curves (3 -4). Reproduced from: Sun J.* Implementation of 2-Step Intensity Modulated Arc Therapy*. Master's thesis. University of Canterbury; 2010. [14]*

For example, treatment planning studies have shown that the maximum dose to the brainstem was reduced by 25–30% in proton plans compared to photon-based SRT, and mean doses to healthy brain parenchyma were reduced by 40–60%, depending on tumor location and beam arrangement [16], [17]. These reductions are clinically significant, particularly in younger patients or those with benign histology, where minimizing long-term toxicity and the risk of secondary malignancies is of critical importance [18].

2. Dose Distribution Quality, Robustness, and LET: Three Competing Aspects in Proton Therapy Plan Optimization

2.1. Physical Principles and Dose Distribution

Among the various forms of radiation therapy, proton therapy is gaining increasing attention due to its unique physical and biological properties. Unlike conventional photon beams, protons exhibit a well-defined dose distribution pattern characterized by the Bragg peak—an effect that allows for maximal energy deposition at a specific depth within tissue. This enables superior dose conformity and reduced exit dose, making proton therapy particularly valuable for treating tumors located near radiosensitive structures [7].

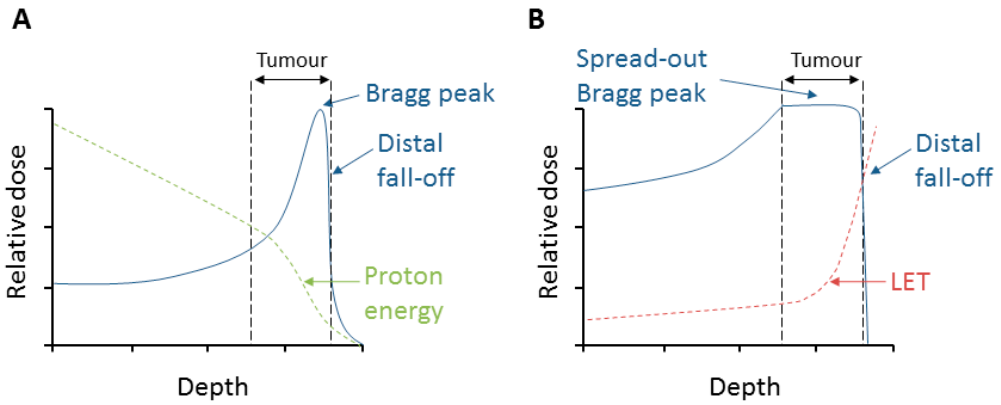

Figure 4. *Depth–dose distribution of protons and relationship to energy and linear energy transfer (LET). (A) An unmodulated (pristine) Bragg peak produced by a proton beam. (B)Spread-out Bragg peak (SOBP) from several modulated proton beams. Reproduced from Vitti E.* Cancers (2019), 11(7), 946, *[7]*

Protons are directly ionizing radiation that primarily interact with matter through multiple Coulomb interactions with the outer-shell electrons of atoms. As they traverse a medium such as water or tissue, protons continuously lose kinetic energy along their path. The average rate of energy loss by protons, known as the stopping power (S), is mathematically expressed as:

$$S = -dE/dx \quad (1)$$

where E is the proton energy and x is the distance traversed by the proton [6]. Equation 1 describes the energy deposited by a proton in the medium per unit path length.

In proton therapy, not only the physical dose but also the linear energy transfer (LET) plays a crucial role in determining the biological impact of treatment. To better assess LET distributions across target volumes and critical structures, LET Dose Volume Histograms (LDVH) are increasingly used. These histograms, analogous to conventional DVHs, provide insights into the spatial distribution of LET values and allow medical physicist to evaluate potential hotspots of elevated biological effectiveness. This approach is particularly relevant when integrating LET-based considerations into treatment planning, since elevated LET in or near normal tissues may enhance biological effects and increase the risk of toxicity, even when the physical dose remains within acceptable limits.

The following subsections provide a detailed discussion of each of these competing factors—beginning with the biological implications of LET and RBE, followed by an analysis of plan

robustness, and concluding with strategies for integrating LET-based optimization into proton therapy planning.

2.2. Relative Biological Effectiveness and LET-Related Uncertainty

One of the key concepts related to the stopping power of particles is LET. As protons travel through matter, they lose kinetic energy, and their LET increases monotonically along the entire penetration path [3]. This implies that the same physical dose delivered at the beam entrance and near the distal edge can result in different biological effects. In particular, higher LET values are generally associated with an increased likelihood of cell death and tissue damage.

This variation in the biological effectiveness of an identical physical dose is described by the parameter known as relative biological effectiveness (RBE). RBE represents the degree of biological response and depends not only on the dose but also on radiation quality, including LET. In practice, this means that the RBE of protons can vary significantly along the beam path—from approximately 1.0–1.1 at the entrance plateau to peak values around 1.7 near the distal edge of the spread-out Bragg peak (SOBP) [3].

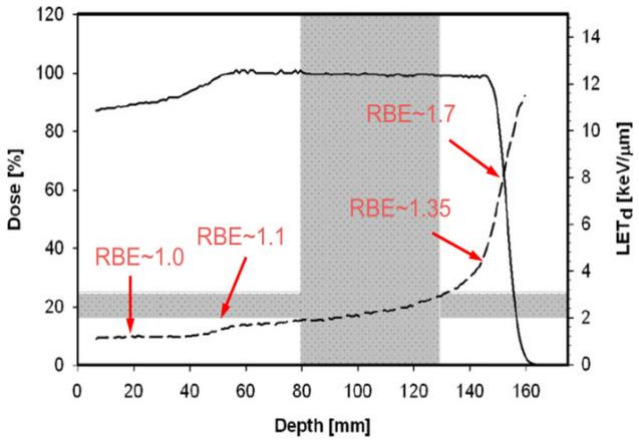

Figure 5. *RBE variation along the length of a spread-out Bragg peak (shaded region). Note the correlation between RBE and LET (dotted line).Reproduced from Paganetti H. Phys Med Biol. 2014;59(22):R419 [3]*

However, most commercially available treatment planning systems (TPS) for proton therapy assume a fixed RBE value of 1.1, applied uniformly across the entire anatomical region. This simplification overlooks the spatial variation of LET and, as a result, may lead to an underestimation of the biologically effective dose in sensitive structures.

As illustrated in ***Figure 6***, LET reaches its highest values in the distal portion of the beam—near the tumor boundary and adjacent organs at risk. This overlap is one of the primary sources of biological uncertainty in proton therapy planning and warrants careful consideration in both complication risk assessment and radiobiological modeling [5], [19]

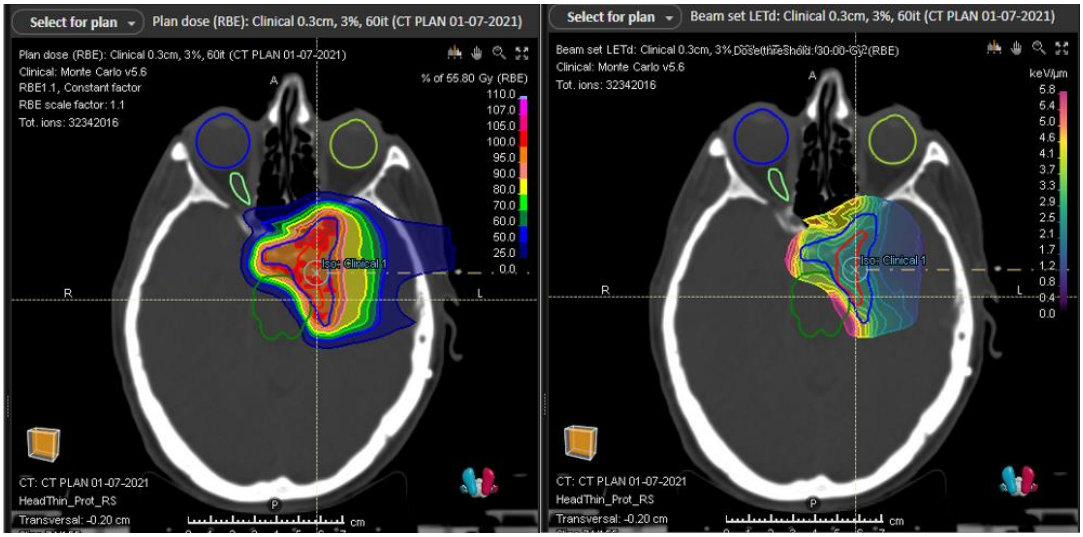

Figure 6. *Spatial distribution of Dose and LET for a proton beam with a spread-out Bragg peak (SOBP): LET increases as the distal edge of the beam is approached.*

Thus, accurate understanding and control of LET distribution in tissues are critical for assessing potential biological effects and for developing robust treatment planning strategies. In recent years, there has been active development of methods that incorporate LET-related parameters into the inverse planning process, particularly for tumors located in close proximity to critical structures.

2.3. LET-Based Optimization in Proton Therapy

Regions of high LET are frequently associated with increased biological effectiveness, which can serve as both a therapeutic advantage and a potential risk for unintended damage to healthy tissue. This underscores the need for reliable LET optimization during treatment planning. By incorporating LET-based constraints and objectives into the optimization process, clinicians aim to preserve the physical precision of proton therapy while mitigating potential biological uncertainties. The following sections of this thesis will explore LET optimization strategies in proton therapy of the brain, with a focus on approaches that

balance tumor coverage with the protection of adjacent critical structures, such as the brainstem.

Despite the well-established physical advantages of proton therapy, an increasing number of clinical reports highlight cases of radiation-induced necrosis in the brain and brainstem following treatment of central nervous system tumors. These adverse effects are typically associated with high doses and the placement of dose peaks near sensitive structures; however, there is growing interest in the role of elevated LET in the development of such injuries.

Clinical data provide support for this hypothesis. In a retrospective study by Bahn et al. (2020) involving patients with low-grade gliomas, a statistically significant correlation was identified between regions of high LET and the occurrence of late contrast-enhancing brain lesions following proton therapy. These findings support the hypothesis that the risk of necrosis may be influenced not only by the absolute physical dose but also by the spatial distribution of LET. Particularly vulnerable regions include areas near the ventricular system and the distal edges of the proton beam, where LET tends to rise sharply and uncontrollably [20].

These clinical observations are supported by biophysical evidence presented in the work of Paganetti et al. (2019) and McMahon et al. (2018), where it is emphasized that high LET can lead to more pronounced tissue damage at equivalent physical doses due to increased relative biological effectiveness (RBE) [21], [22]. McMahon and colleagues also demonstrated that incorporating LET-weighted dose calculations can reduce biological effect variability in treatment plans and potentially provide better predictions of high-risk regions.

In response to these challenges, LET-based planning approaches have been proposed in recent years. According to Hahn et al. (2022), the incorporation of LET constraints into IMPT optimization algorithms enables the displacement of high-LET regions away from critical structures, including the brainstem, thereby reducing the likelihood of late complications without compromising target coverage [23]. Their study compared various biologically guided optimization strategies, with the best outcomes achieved when both dose and LET were evaluated simultaneously.

Taken together, the accumulated clinical and theoretical data support the need to integrate LET parameters into the planning process for brain tumor treatments. LET optimization, in particular, is emerging as a promising tool for minimizing the risk of radiation necrosis, especially in cases where the tumor is located near the brainstem or other critical structures.

With the increasing integration of biologically relevant physical parameters—such as LET—into treatment planning algorithms, leading treatment planning systems have begun to implement corresponding LET optimization tools. One of the first commercial implementations was introduced in RayStation (RaySearch Laboratories), which offers two types of LET-based optimization:

1. MaxLETd – This method aims to reduce the dose-averaged LET (dose-averaged LET) within selected structures. It is primarily used to limit the biological impact on critical organs located near the target volume, such as the brainstem or cerebral cortex.
2. MaxLVH – This strategy utilizes the LET-volume histogram (LVH) function to constrain the volume of tissue receiving LET values above a defined threshold. It provides more precise control over the spatial distribution of high-LET regions, particularly when intersecting with radiosensitive areas of the brain [23].

The main difference between these two approaches lies in the objective function: MaxLETd minimizes the average LET within anatomical structures, while MaxLVH targets the volume distribution of LET, limiting the proportion of tissue exposed to LET values above a critical level.

In this study, the MaxLVH strategy was selected for plan optimization, as it was deemed more suitable for restricting high-LET regions in the brain and brainstem, particularly when aiming to comply with predefined threshold values. This method was applied in combination with clinical dose constraints and was used consistently throughout all re-optimization stages.

2.4. Uncertainties in Proton Therapy

Traditional planning approaches - such as the use of a planning target volume (PTV) - do not fully account for the sensitivity of proton therapy to various clinical and physical uncertainties. According to ICRU Report 83, the target volumes are defined as follows: Gross Tumor Volume

(GTV) refers to the visible or palpable extent of disease, Clinical Target Volume (CTV) includes the GTV and regions with potential microscopic spread, and Planning Target Volume (PTV) adds margins to the CTV to compensate for uncertainties in setup and range [24].

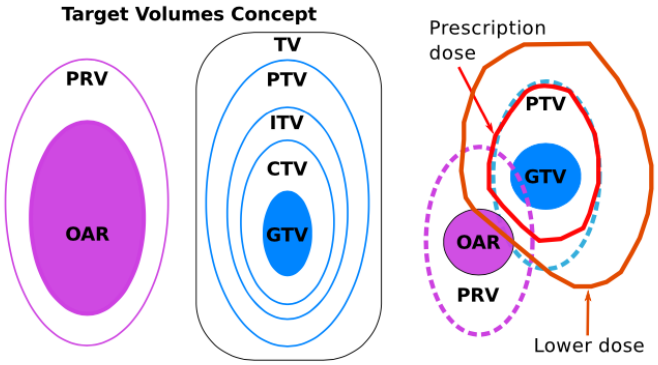

Figure 7. *Visual representation of target volume concepts in radiation therapy, including GTV, CTV, PTV, PRV, and OAR. Reproduced from Schlachter M, Raidou RG, Muren LP, et al. Comput Graph Forum. 2019;38(3):753–779 [25]*

However, such an approach is not sufficient in the context of intensity-modulated proton therapy (IMPT). Due to the steep distal fall-off of proton dose distributions, treatment plans are typically optimized directly on the CTV without introducing a PTV. As a result, IMPT becomes highly sensitive to both systematic and random deviations, such as setup errors (typically ±3 mm), proton range uncertainties (commonly estimated as ±3.5%) [26], inaccuracies in CT-to-stopping-power conversion, CT imaging artifacts, and anatomical changes between treatment fractions [27], [28], [29], [30]. If these factors are not properly accounted for, dose distributions calculated under nominal conditions may significantly degrade in actual clinical practice [31], [32]

To address these issues, modern IMPT planning incorporates robust evaluation techniques. Rather than relying on geometric safety margins, robust optimization assesses the stability of both dose and LET distributions across a set of clinically justified perturbation scenarios. These typically include translational uncertainties along the three orthogonal axes and proton range deviations. Optimization is performed simultaneously on the nominal CT and the perturbed CTs, ensuring that treatment goals—such as target coverage and OAR sparing—are met under all conditions.

In practice, evaluation may involve voxel-wise analysis, where the worst-case scenario is considered for each voxel. In most clinical workflows, plan approval is primarily based on inspection of the dose distribution on the nominal CT and secondarily on its robustness across uncertainty scenarios. To facilitate interpretation, dose–volume histogram (DVH) bands are commonly used. These bands illustrate the variability of dosimetric parameters across scenarios. The width of these bands at key DVH points—such as D95 for the CTV or Dmax for an OAR—serves as a quantitative measure of plan robustness.

An example of this approach is illustrated in ***Figure 8***, which shows DVH curves calculated for a set of uncertainty scenarios. The figure demonstrates how dosimetric parameters vary with changes in patient positioning and proton range, enabling evaluation and quantitative comparison of the robustness of different treatment plans.

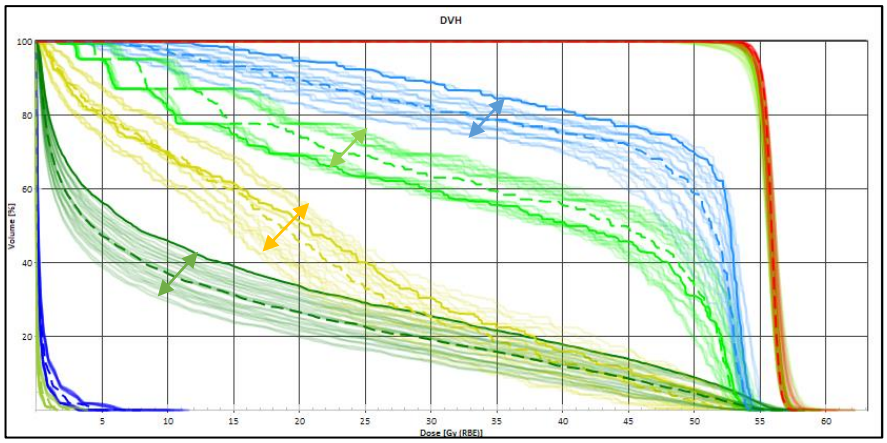

Figure 8. *Example of DVH-based robust evaluation under setup and range uncertainties. The width of the DVH bands reflects the sensitivity of the CTV and critical organs to different uncertainty scenarios.*

To actively mitigate the impact of uncertainties, robust optimization techniques are applied. Instead of optimizing for a single nominal scenario, these algorithms simultaneously consider a predefined set of perturbed scenarios and search for a solution that performs adequately across all of them. A widely adopted strategy is voxel-wise worst-case optimization, where the minimum dose across scenarios is used for target voxels, while the maximum dose is applied to voxels in organs at risk [30], [31]. This approach enhances plan robustness and reduces the risk of clinically significant deviations during treatment delivery.

2.5. The “Trilemma” of Proton Therapy Planning

Incorporating LET objectives into treatment plan optimization offers promising opportunities to enhance the biological effectiveness of proton therapy, particularly in hypoxic or radioresistant tumors. However, it also introduces a set of competing priorities. As demonstrated in a recent study by Fredriksson et al. [33], there is an inherent conflict between achieving robust target coverage, maintaining uniform dose distribution, and maximizing dose-averaged LETd within the tumor.

For an in-silico study on digital phantoms, they evaluated the impact of range and setup uncertainties on the achievable LETd levels for targets of varying sizes under robust optimization scenarios. It was shown that increasing range uncertainty from 0% to 5% resulted in a 17–29% reduction in near-minimum nominal LETd (equivalent to 9–21 keV/µm), while setup uncertainties had a smaller yet non-negligible impact. This highlights a fundamental trade-off: optimizing for high LETd often compromises plan robustness, and vice versa [33].

Moreover, the study indicated that permitting a certain degree of dose escalation—either within the gross tumor volume (GTV) or the clinical target volume (CTV)—can help mitigate this conflict. For example, allowing a 10% dose increase in the GTV enabled worst-case LETd values to rise by 1–8 keV/µm, depending on tumor size. However, such approaches carry inherent risks, including potential overdose to adjacent healthy tissues if uncertainties are underestimated. In other words, it may not be feasible to simultaneously maximize all three objectives for larger tumors, making clinical prioritization and careful planning essential [33].

Therefore, given the inevitable tension between physical dose conformity, plan robustness, and biological parameters, LET distribution optimization requires a balanced and context-aware approach. In the present work, particular emphasis is placed on identifying compromise solutions that accommodate these competing demands in the planning of proton therapy for brain tumors.

3. LET Optimization in Proton Therapy for Brain Tumors to Reduce Side Effects

In radiation therapy, side effects also known as radiation-induced toxicities refer to unintended damage to healthy tissues that results from therapeutic radiation. These effects

can be acute -occurring during or shortly after treatment or late - manifesting months or years later, and are commonly graded using standardized scales. Grading typically ranges from Grade 1 (mild) to Grade 5 (fatal), based on severity and clinical impact. OARs are classified as either serial or parallel, depending on their functional structure and tolerance to radiation. Serial organs, such as the spinal cord and brainstem, are highly sensitive to localized high-dose exposure, damage to even a small segment can result in significant loss of function. In contrast, parallel organs, such as the lungs or liver, can tolerate higher doses to small sub-volumes as long as the overall mean dose remains low. Therefore, treatment planning aims to minimize the maximum dose for serial organs and the mean dose for parallel organs [2].

For each organ, dose constraints are typically derived from clinical data that relate specific dose thresholds to the probability of a given side effect. These constraints serve as acceptable risk levels, guiding the prescription of safe and effective treatments. In recent years, efforts have been made to identify analogous thresholds for LET, particularly in proton therapy, where variable LET distributions can influence biological outcomes [34], [35], [36], [37].

However, LET values alone are not predictive of tissue damage. Their impact must be considered in combination with dose and volume to reflect the actual risk of toxicity. Consequently, many current studies focus on correlating high-LET, high-dose, and high-volume regions with observed complications, especially in critical areas.

In the context of intracranial proton therapy, particular attention is paid to OARs in the brain and brainstem, which are located in close proximity to many common tumor types such as meningiomas, ependymomas, and brain metastases. These structures are functionally serial and highly radiosensitive, making them particularly vulnerable to adverse effects from elevated LET and/or high-dose exposure.

Based on these considerations, the following section explores clinical and dosimetric studies that have investigated threshold values for dose, LET, and volume associated with increased toxicity in these regions, with the goal of improving LET-based planning strategies in proton therapy.

3.1. Analyzing possible correlation between dose, LETd values and the incidence of side effects in organs at risks

A recent retrospective study conducted at the National Center for Oncological Hadrontherapy (CNAO, Pavia) analyzed the relationship between dose, LET, and the development of brain necrosis in 124 patients treated with intensity-modulated proton therapy (IMPT) for intracranial meningiomas and solitary fibrous tumors [34].

The authors employed the dose-LET-volume histogram (DLVH) analysis method to assess the dose-LET-dependent characteristics within out-of-target brain regions. The analysis revealed that the most significant predictor of radiation necrosis was the volume of brain tissue receiving a Dose > 42.9 Gy(RBE) combined with a dose-averaged LET (LETd) > 4.6 keV/µm. In patients who developed necrosis, the median volume of such regions was 8.2 cm^3, compared to 1.1 cm^3 in those without complications. Multivariate analysis confirmed that this combined metric was statistically significantly associated with the risk of complications.

Based on these findings, the following OAR constraints were adopted in this thesis to guide LET optimization for the healthy brain:

- LET ≥ 4.6 keV/µm,
- Dose ≥ 43 Gy (RBE),
- Volume ≤ 1 cm^3.

In addition to retrospective clinical data linking elevated LET values with the development of radiation necrosis, recent years have seen the publication of several multicenter studies aimed at quantifying acceptable LET thresholds in the brainstem region during proton therapy for pediatric posterior fossa tumors.

In a European multicenter treatment planning comparison conducted by Lægdsmand et al. (2024), it was demonstrated that different proton therapy centers generated markedly different LET distributions in the brainstem, despite achieving similar target coverage. This finding highlights the sensitivity of LET to beam geometry and optimization strategies, as well as the need for standardized LET constraints to better protect critical structures [35].

Further important insights were provided by Handeland et al. (2023), who developed LET-inclusive NTCP models to estimate the risk of brainstem necrosis in pediatric patients with ependymoma undergoing proton therapy. Based on their analysis, they proposed limiting

brainstem volumes receiving LET values exceeding 2.5–3.5 keV/µm in combination with high doses (54 Gy[RBE]), as such regions were most frequently associated with the onset of severe symptomatic toxicity [36]. The proposed models showed high predictive accuracy and may serve as valuable tools for clinical decision-making.

These findings were corroborated by the case-control study of Fjæra et al. (2022), which analyzed instances of severe brainstem toxicity in pediatric patients treated with proton therapy. The authors found a significant correlation between increased volumes receiving LET >2.5 keV/µm and the occurrence of symptomatic complications, reinforcing the need to establish LET constraints in organs at risk—particularly when high doses and distal target locations are involved [37].

A review of the available literature indicates that threshold values for LET, dose, and volume associated with brainstem injury vary across studies. This variability can be attributed to differences in treatment planning protocols, beam configurations, patient age groups, and toxicity assessment criteria. Nevertheless, several authors emphasize that even relatively small volumes (≈1 cm^3) exposed to doses ≥50 Gy(RBE) and LET levels exceeding 2.5–2.8 keV/µm may carry a significant risk of symptomatic toxicity, particularly in pediatric patients [35], [36], [37].

In this study, the most conservative thresholds reported in the literature—those associated with adverse clinical outcomes—were adopted to guide the design and evaluation of LET-based strategies:

- LET ≥ 2.8 keV/µm
- Dose ≥ 50 Gy(RBE)
- Volume ≥ 1 cm^3

The use of these values is intended to ensure high sensitivity of the model to potential risks while facilitating the development of planning methods that prioritize maximum protection of the brainstem.

The main findings of these studies are summarized in ***Table 1***, which compiles the reported threshold values of LET, dose, and volume associated with the risk of radiation necrosis in both the brain and brainstem tissues.

Structure	LET (keV/µm)	Dose (Gy RBE)	Volume	Clinical Context	Reference
Brain	> 4.6	>42.9	≥ 1-5cc	Brainstem necrosis following proton therapy	Bazani et al.[34]
Brainstem	2.8–3.6 (median 3.3) 2.5-2.8 (median 2.7)	> 50	—	Complications in the brainstem and upper spinal cord due to high doses after radiotherapy for posterior fossa tumors in children	Lægdsmand et al. [35]
Brainstem	≥ 2.8-3.5 (median 3.1) ≥ 2.9-3.8 (median 3.4)	≥ 54	≥ 10% ≥ 0.1cc	Symptomatic Brainstem toxicity following pediatric proton therapy	Fjæra et al. [37]
Brainstem	≥ 2.33 ≥ 3.80	≥ 54	≥ 10% (4.0% in ntcp curve) ≥ 10% (7.7% in ntcp curve)	Brainstem necrosis following proton therapy of paediatric ependymoma	Handeland et al. [36]

Table 1. *Summary of literature-based constraints for radiation-induced necrosis in the brain and brainstem*

4. Project Aims

The primary objective of this master's thesis is to identify potential optimization strategies for reducing LETd values in healthy organs without significantly compromising the overall plan quality in terms of dose coverage and robustness. This involves evaluating trade-offs between dose conformity, plan robustness, and LETd distribution in the brain and brainstem through the re-optimization of clinical treatment plans for brain tumors.

Despite the relevance of this issue, LET remains a secondary parameter in current clinical practice, as its clinical significance and methods of control are still under investigation and discussion in the scientific community. In this study, we explore the potential clinical impact

of integrating LET optimization into the treatment planning workflow for proton therapy of brain tumors. Modern commercial treatment planning systems (TPS) now offer functionality for LET optimization alongside conventional dose optimization. However, despite the recognized importance of LET control in the literature, a consensus on reference LET values (e.g., LET levels corresponding to specific isodose levels) for guiding clinical decision-making has not yet been established. As a result, LET has not been widely adopted as a routine parameter in everyday clinical practice.

To address this research gap and explore the feasibility of integrating LET-optimized treatment planning strategies into clinical workflows, this thesis is structured around the following specific objectives:

Objective 1: LETd Optimization for the Brain

Retrospective Analysis: based on a comprehensive retrospective analysis of a cohort of patients who developed brain toxicity after treatment at CNAO [34], determine the NTCP curve by correlating specific volume of brain that received a certain LET value with observed toxicity instances.

Re-optimization with Brain LETd Constraints: To implement brain necrosis-related LETd constraints into the initial clinical plans for re-optimization, with the aim of aligning treatment parameters with established baselines to potentially reduce the risk of brain necrosis. The plans will be re-optimized multiple times using different LETd-based optimization strategies.

LETd Variation Impact: Assess the impact on plan dose distribution quality and robustness of LETd variations or the volume receiving a specific LETd value on the NTCP. This evaluation will help quantify optimal LETd (and/or volumes receiving specific LETd value) optimization goals for clinical treatment planning, based on the expected impact on dose conformity and plan robustness due to LETd adjustments.

LETd-Based Re-optimization Using Gantry Geometry: Create an alternative plan using gantry-based geometry instead of the clinical fixed-beam plan using 2–3 fields, using LETd constraints for brain and brainstem to balance dose conformity, robustness, and LETd distribution.

Objective 2: LET Optimization for the Brainstem

Literature Review: Conduct review of relevant literature to identify LETd volume-dose parameters specifically linked to toxicities in the brainstem. This review will support the establishment of evidence-based LETd thresholds for subsequent treatment plan optimizations.

Re-optimization with Brainstem LETd Constraints: Utilizing the insights gained from the literature review, integrate the derived LETd constraints for the brainstem into the clinical plans for re-optimization. Similar to the approach for the brain, evaluate the impact of LETd variations on the plan's dose conformity and robustness for the brainstem. Additionally, combine LETd optimization for the brainstem with previously identified objectives for the brain.

LETd-Based Re-optimization Using Gantry Geometry: Create an alternative plan using gantry-based geometry instead of the clinical plan with a fixed beam geometry of 2-3 beams plan, using LETd constraints for brain and brainstem to balance dose conformity, robustness, and LETd distribution. Together, these objectives aim to establish practical and clinically relevant guidelines for LET-aware planning in brain tumor proton therapy.

Ultimately, the resulting plans will be comprehensively evaluated according to three key aspects: dose distribution quality, LETd maps, and robustness to clinically relevant uncertainties. This analysis will enable the identification of optimal trade-offs among these competing factors within a realistic clinical workflow for brain tumor treatment planning. Finally, the potential reduction in radiation-induced side effects in healthy tissue will be quantitatively assessed for the newly optimized plans generated using different LETd optimization strategies, based on a previously developed NTCP model.

Methods and materials

1. Patient Cohort and Clinical Data

In this study, we selected twenty patient treated between 2018 and 2025 at the CNAO using proton therapy. All patients received a prescribed dose of 55.8 Gy, delivered in 31 fractions of 1.8 Gy. Patient were selected in order to have the same fractionation scheme, based on the most common in clinical practice. Most of the patients within this group were diagnosed with grade I–II meningioma and adamantinomatous craniopharyngioma. Moreover, as discussed in the previous chapter, the risk of developing brain and brainstem necrosis has been associated with dose levels in the range of 43–50 Gy, which fall within the considered dose range. In this type of treatments, the target volume (CTV) was located in close proximity to the brainstem. No specific selection based on target volume was performed, as one of the study objectives was to evaluate the feasibility of LET optimization across a range of CTV sizes. The CTV volume varied from 5.25 cm^3 to 123.18 cm^3, with a median value of 40.12 cm^3.

Since clinical plans serve as the reference standard in this study, this section describes their generation and the methodology used for robustness evaluation, as these plans will later be compared to alternative optimization approaches. Among the 20 analyzed clinical plans: 9 plans used 2 irradiation fields, 10 plans used 3 fields, and 1 plan included 4 fields. All beams were arranged coplanarly, meaning they lay within the same plane, with beam directions varied by rotating the treatment couch.

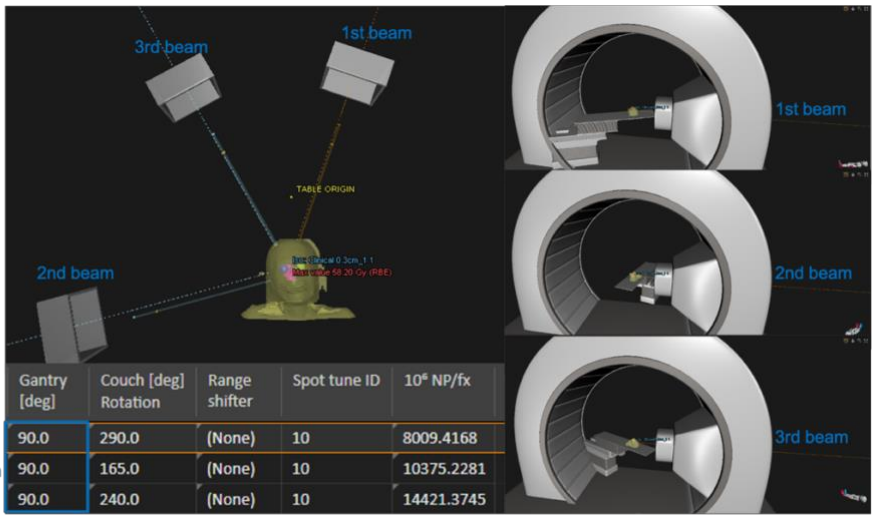

	Gantry [deg]	Couch [deg] Rotation	Range shifter	Spot tune ID	10^6 NP/fx
1st beam	90.0	290.0	(None)	10	8009.4168
2nd beam	90.0	165.0	(None)	10	10375.2281
3rd beam	90.0	240.0	(None)	10	14421.3745

***Figure 9**. Example of coplanar beam arrangement in a clinical plan*

Plan optimization was performed using the RayStation treatment planning system with robust optimization enabled. The uncertainty parameters were as follows:

- Patient positioning uncertainty: ±0.3 cm
- Systematic tissue density uncertainty: ±3%
- A total of 21 uncertainty scenarios were evaluated.

Given that these clinical plans were implemented in real patient treatments, the prescribed dose distributions and clinical goals were met, and the plans were not altered within the scope of this research.

LET analysis was performed using the LVH script**,** which allows the selection of a specific structure and determines the LET value at a given dose and volume.

The Robust Evaluation was carried out considering the most common clinical uncertainties that can affect dose distribution and LET profiles. The calculations accounted for a patient positioning uncertainty of ±0.2 cm, reflecting possible daily setup variations. Additionally, a systematic uncertainty of ±3% in tissue electron density was modeled, corresponding to deviations that may arise during CT contouring and the conversion of Hounsfield units to density. A three-point discretization approach was used to represent all possible combinations of these two factors, resulting in 24 uncertainty scenarios that cover a realistic range of clinical variability.

The robust evaluation focused on three main aspects. First, the coverage of the CTV and its consistency across all scenarios were analyzed. Second, maximum dose values within the CTV were evaluated, as they are critical in terms of the risk of necrosis. Finally, special attention was given to the dose delivered to critical structures selected for LET optimization — the brain and the brainstem.

For the CTV, clinical thresholds were used as reference criteria:

- ≥ 53.01 Gy (95% of the prescribed dose) to 95% of the volume;
- ≥ 54.68 Gy (98% of the prescribed dose) to 98% of the volume;
- ≤ 57.47 Gy (103% of the prescribed dose) to 1% of the volume.

For the organs at risk, the dose limits were:

- ≤ 57.47 Gy (103% of the prescribed dose) to 1 cm^3 of the Brain;
- ≤ 55.80 Gy (100% of the prescribed dose) to 1 cm^3 of the brainstem.

Plan comparisons across all 24 scenarios enabled a quantitative assessment of how the proposed LET optimization affects adherence to these thresholds and the overall robustness of the dose distribution.

2. Definition of Substructures and LET Constraints

The parameters for LET optimization were initially derived from retrospective analyses. Plans that, after the first round of optimization, maintained adequate coverage—defined as greater than 96% of the prescribed dose—were subsequently re-optimized with increasingly stricter LET constraints until the coverage dropped below clinically acceptable levels, i.e., less than 95% of the prescribed dose. Optimization was performed simultaneously for both the brain and the brainstem.

To visualize the overall structure of the plan generation process and the application of LET constraints, the workflow is summarized in ***Figure 10.***

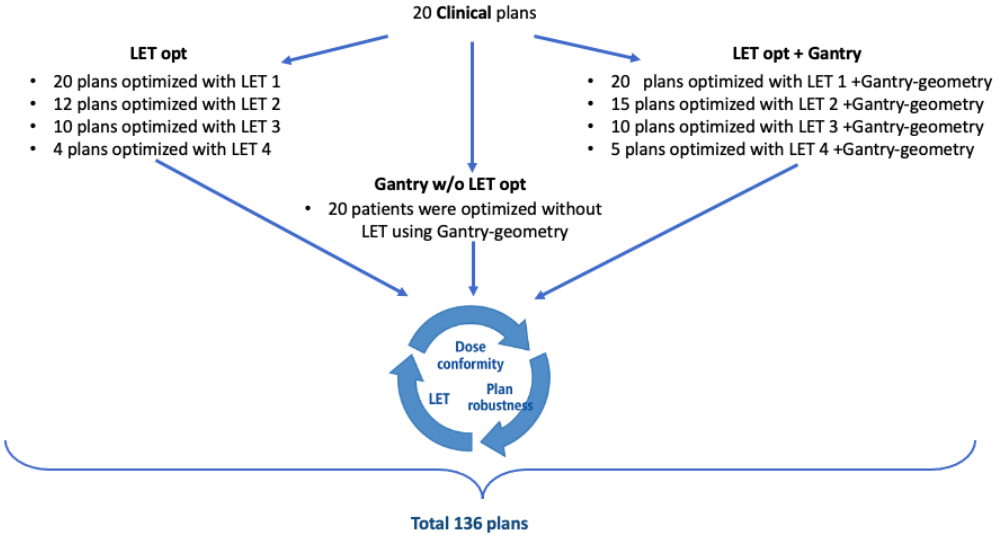

Figure 10. *Overview of the study workflow and distribution of LET-optimized plans.*

Constraints were applied to specially developed auxiliary control structures, designed to increase the weight of LET constraints for both the brain and brainstem. The selection of these structures and the corresponding constraint parameters was based on empirical evaluation to optimize LET in a way that achieved the desired outcomes.

During the optimization process, it was found that due to the large volume of the Brain structure (average 1244.5 cm^3), the relative weight of the constraint was too small. In order to apply a constraint to 1 cm^3, the corresponding volume would need to be set as 0.07% of the total, or even less, which led to ineffective LET reduction in the brain.

As a result, a new auxiliary structure named **"Brain opt"** was created. It was generated using the intersection tool between the Brain-GTV (i.e., the whole brain volume excluding the GTV volume) and the GTV expanded by 3 cm, yielding an average volume of approximately 307.2 cm^3 ***Figure 11***.

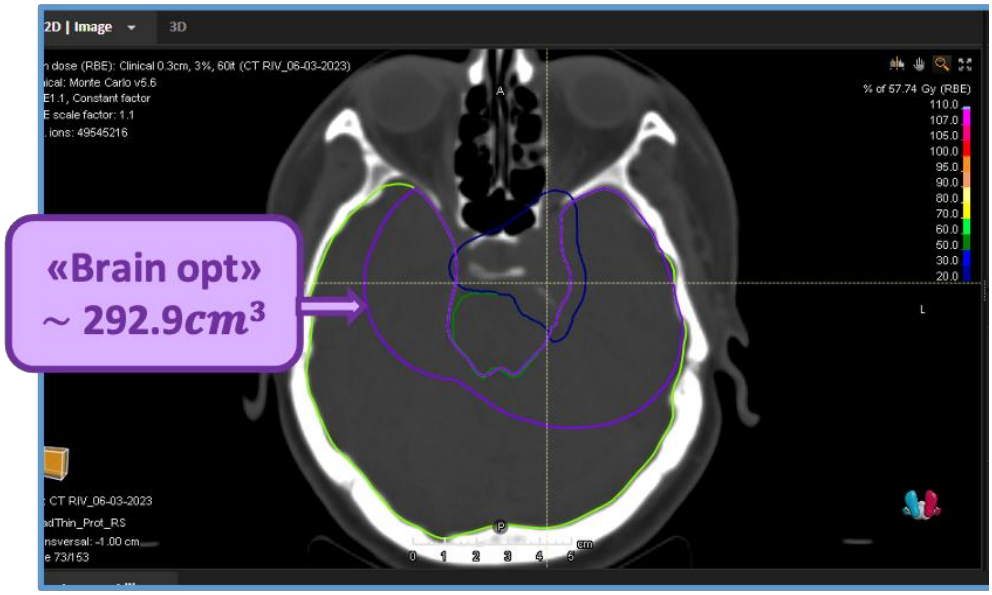

Figure 11. *Parameters for the creation of the "Brain opt" structure and its volume*

For the brainstem, which had an average volume of 27.4 cm^3, an additional structure was created to increase the relative weight of the LET constraint. This structure was developed based on the clinical plan, considering the LET distribution (2.8 keV/µm) and a dose corresponding to 84% of the prescribed value (47 Gy). It was generated using an intersection tool to combine the regions within the brainstem that met these criteria, followed by exclusion of the GTV with a 0.1 cm margin. The resulting structure, named "Brainstem opt",

had a volume of 2.4 cm³. The approaches for creating these two additional structures were empirically derived through testing different tools and techniques.

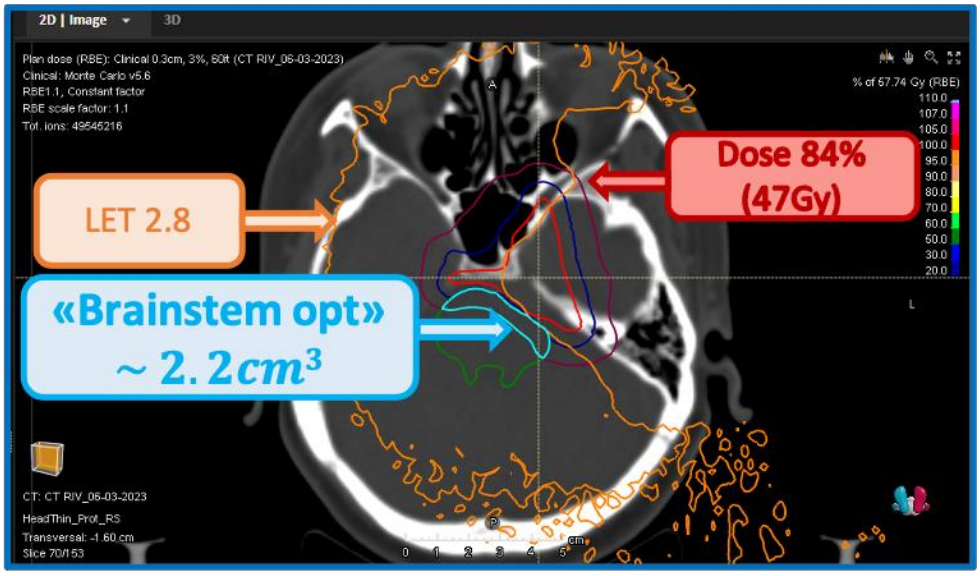

Figure 12. *Parameters used for the creation of the "Brainstem opt" structure and its volume*

The parameters for each optimization approach are summarized in ***Table 2***.

	1 LET Opt	*2 LET Opt*	*3 LET Opt*	*4 LET Opt*
Brainstem	2,5keV/nm, 50Gy, 5%	2keV/nm, 50Gy, 3,5%	1,5 keV/nm, 50Gy, 2%	1 keV/nm, 50Gy, 1%
Brain	4,6 keV/nm, 43Gy, 0,3%	4,2 keV/nm, 43Gy, 0,3%	3,8 keV/nm, 43Gy, 0,3%	3,4 keV/nm, 43Gy, 0,3%

Table 2. *Parameters for LET Optimizations 1–4 (LET Opt)*

3. Planning Approaches

3.1. Planning Approaches with LET Optimization

As part of the LET optimization process, the clinical plan was first duplicated. LET constraints were then applied to the brain (Brain opt) and brainstem (Brainstem opt). Following the introduction of these constraints, optimization was performed, during which the final dose distribution was calculated.

Once dose calculation was complete, target coverage (CTV) was assessed. If the coverage exceeded 95% of the prescribed dose, LET values were analyzed using the LVH script: for the

brain at 43 Gy and 1 cm^3 volume, and for the brainstem at 50 Gy and 1 cm^3. A robust evaluation was subsequently carried out using the same uncertainty parameters as in the clinical plan. This process was performed for all 20 patients.

Then further optimization was carried out using increasingly stricter LET constraints. The process followed the same methodology as the initial optimization, with the only difference being the adjustment of constraint parameters for the relevant structures.

3.2. Gantry-Based Planning Approaches With and Without LET Optimization

As part of this section of the study, an alternative treatment plan using a non-coplanar beam geometry was created for each patient. This approach simulates the use of a gantry, which is currently in the installation phase at CNAO. In the near future, the gantry system is expected to be integrated into routine clinical treatment planning. Meanwhile, gantry geometry is already available for use in treatment plan optimization within the TPS. In this context, the outcomes of the present study will provide valuable practical insights and may serve as a foundation for the clinical implementation of gantry-based treatment planning within the framework of the new system.

The number and orientation of the beams were determined individually based on the shape and location of the target volume and were reviewed and approved by an experienced clinical medical physicist.

A total of 20 gantry-based plans were generated, with the number of irradiation fields distributed as follows: 2 fields in 5 cases, 3 fields in 14 cases, and 4 fields in 1 case.

In most plans, a combination of one coplanar and two non-coplanar beams was used, providing greater flexibility in managing LET and dose distribution near critical structures ***Figure 13.***

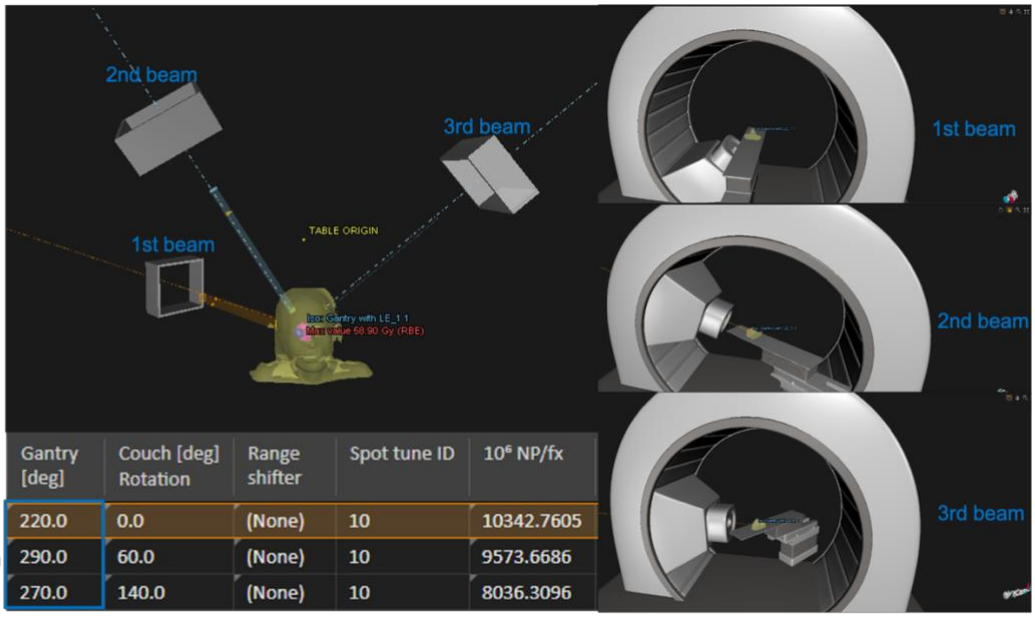

	Gantry [deg]	Couch [deg] Rotation	Range shifter	Spot tune ID	10^6 NP/fx
1st beam	220.0	0.0	(None)	10	10342.7605
2nd beam	290.0	60.0	(None)	10	9573.6686
3rd beam	270.0	140.0	(None)	10	8036.3096

Figure 13. *Example of non-coplanar beam arrangement in gantry-based plans*

To improve dose shaping and reduce unnecessary low-dose spread around the target volume, additional ring structures were created. These structures were specifically used during the optimization process to limit dose distribution in peripheral regions.

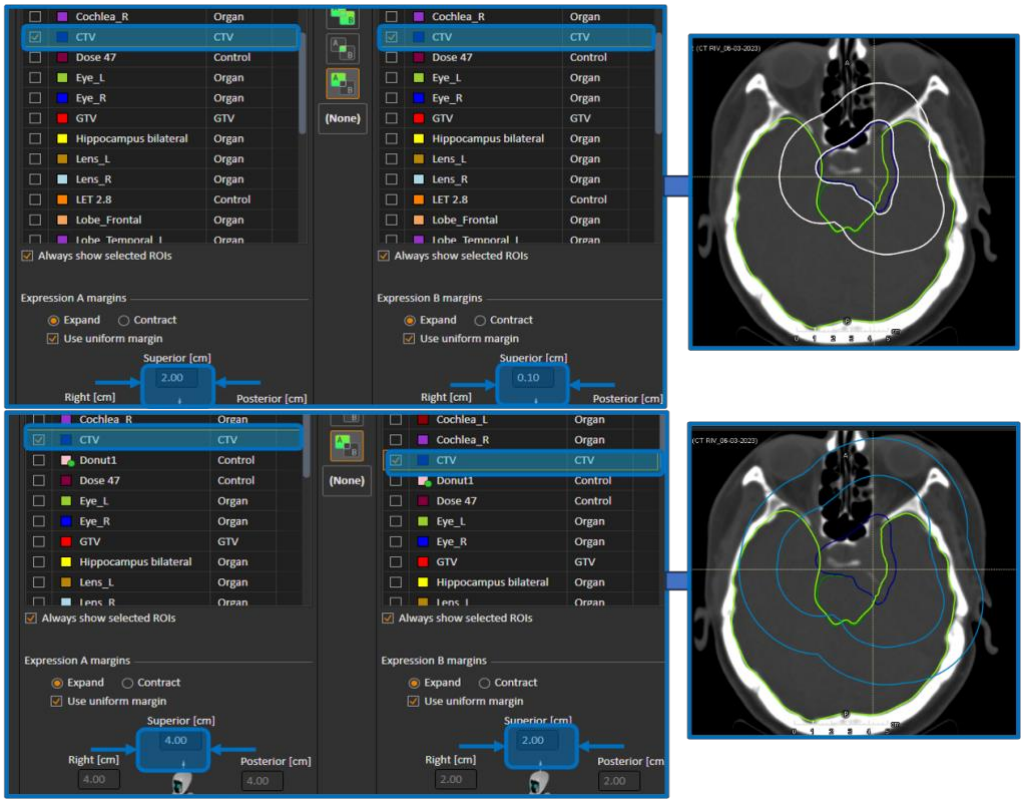

Figure 14. *Example of additional ring structures and their creation parameters*

For the gantry-based plans, the objective was to achieve dose values comparable to those of the clinical plan. In other words, the critical structures were required to receive approximately the same mean doses as in the corresponding clinical plans for each individual patient. The constraint parameters for each optimization approach are presented in ***Table 3***.

	Gantry w/o LET Opt	Gantry +LET Opt 1	Gantry +LET Opt 2	Gantry +LET Opt 3	Gantry +LET Opt 4
Brainstem	-	2,5keV/µm, 50Gy, 5%	2keV/µm, 50Gy, 3,5%	1,5keV/µm, 50Gy, 2%	1keV/µm, 50Gy, 1%
Brain	-	3,8keV/µm, 43Gy, 0,3%	3,4keV/µm, 43Gy, 0,3%	3keV/µm, 43Gy, 0,3%	2,6keV/µm, 43Gy, 0,3%

Table 3. *LET constraint parameters for gantry-based LET optimization approaches 1–4*

As part of this gantry-based planning approach, five separate plans were created for each patient. The first plan was generated without any LET constraints and served as the baseline. Subsequently, plans were developed with the application of LET constraints at levels 1, 2, 3, and 4, resulting in a total of five distinct gantry-based planning strategies per patient.

The LET constraint parameters for the brain in these plans differed from those used in the non-gantry LET optimization approaches, as the initial LET values in gantry-based geometries were already below the established threshold for this structure. To assess the impact of gantry-based geometry on the dose delivered to healthy tissues, an additional structure was created. This structure encompassed the patient's body up to the level of the chin, excluding the target volume without any margins, and was labeled "Health Tissue - CTV". It was used to analyze the mean dose received by healthy tissues, excluding the target area.

To assess the spatial quality of the dose distribution, two key metrics were evaluated: the Conformity Index (CI) and the Homogeneity Index (HI). These indices were computed for all optimization approaches, including the Clinical plan, LET-optimized plans, and Gantry-based plans.

Conformity Index (CI) quantifies how well the prescription isodose conforms to the target volume. It is calculated as the ratio between the volume of the target structure covered by the isodose ($V_{coveredTarget}$) and the total volume enclosed by the isodose surface ($V_{isodose}$). An

ideal *CI* value is close to 1, indicating that the isodose volume closely matches the target shape and size.

$$CI = \frac{V_{Covered\ Target}}{V_{Isodose}} \quad (2)$$

Homogeneity Index (HI) measures how evenly the dose is distributed within the target. It is defined as the ratio of the dose received by 98% of the target volume (D98%) to the dose received by 2% of the volume (D2%). A *HI* value close to 1 indicates uniform dose distribution, whereas lower values indicate the presence of hot or cold spots.

$$HI = \frac{D(x)}{D(100-x)} \quad (2) \text{ where } x=98 \rightarrow HI = \frac{V_{98\%}}{V_{2\%}} \quad (3)$$

Dose and LET Values Analysis

For each plan, the following parameters were calculated:

- LET optimization for the brain and brainstem was performed using different constraint
- Robust evaluation was conducted for each plan, including:
    - For the CTV: D95%, D98%, and D1% (hotspot)
    - For the organs at risk: D1cc for the brain and brainstem.

Then, the following data were extracted:

- D95% for the target (CTV) and D1cc for the brain and brainstem (from DVHs).
- LET values for the brain at a volume of 1 cm^3 at 43 Gy, and for the brainstem at volumes of 1 cm^3 and 0.5 cm^3 at 50 Gy (from LVHs).
- The percentage of scenarios meeting each criterion and the dose in the worst-case scenario (from Robust Evaluation).

This analysis cycle was repeated for all plan groups: with different levels of LET optimization, with gantry-based geometry combined with LET optimization, and with gantry-based geometry without LET optimization. The next level of LET constraints was applied only if the CTV coverage (D95%) remained within clinically acceptable limits (≥ 95%).

Results

A total of 136 treatment plans were analyzed, developed using clinical data from 20 patients. These plans were classified into the following groups:

1. Clinical plans: 20 original reference plans used as the baseline for comparison.

2. LETd-optimized plans:

- 20 plans with a single LETd constraint — "1 LET opt",
- 12 plans with two LETd constraints — "2 LET opt",
- 10 plans with three LETd constraints — "3 LET opt",
- 4 plans with four LETd constraints — "4 LET opt".

3. LETd-optimized plans with gantry-based beam geometry:

- 20 plans — "Gantry + LET opt 1",
- 15 plans — "Gantry + LET opt 2",
- 10 plans — "Gantry + LET opt 3",
- 5 plans — "Gantry + LET opt 4".

4. Plans without LETd optimization but with gantry-based geometry: 20 plans — "Gantry w/o LET opt".

All plans were evaluated based on the following key criteria:

1. Dose distribution plan quality: adequate target coverage, reduced dose to OARs, target CI, target HI, dose to the healthy tissue.
2. Plan LET distribution: the distribution of LET, in particular the LET at a specific dose (relevant for clinical plans) for a specific volume.
3. Plan robustness: the capability of the plan to maintain the nominal characteristics in terms of dose/LET distribution under scenarios of possible clinical uncertainties.

These parameters were used to perform a comprehensive assessment of the effectiveness of each planning strategy.

1. Dose distribution analysis

Clinical plans: The average target coverage relative to the prescribed dose of 55.8 GyE across the cohort of 20 patients was 97.3% ± 1.2% (mean ± standard deviation). To evaluate the maximum dose to organs at risk, the dose to 1 cm^3≥ of volume (D1cc) was used as a metric. The clinical valued D1cc was 52.9 GyE ± 1.4 GyE for Brainstem, and Brain - 56.3 GyE ± 0.5 GyE.

After LETd optimization «1 LET Opt»: Optimization led to a 1% reduction in target coverage—from 54.3 GyE ± 0.7 GyE (97.3% ± 1.2%) to 53.7 GyE ± 0.5 GyE (96.3%± 1,0%). Nevertheless, all plans remained clinically acceptable, meeting the D95 = V95 criterion. The maximum dose to optimized structures, evaluated using the D1cc metric, showed a 5.2% decrease for the brainstem (from 52.9 GyE to 49.8 GyE). For the brain, a slight increase of 0.3% was observed (from 56.3 GyE to 56.4 GyE).

The results of the subsequent LETd-optimized plans (2–4 LET opt), LETd-optimized plans with gantry-based beam geometry (Gantry + LET opt 1–4), and plans without LETd optimization but with gantry-based geometry (Gantry w/o LET opt) are presented in ***Table 4***.

Clinical plans			
Dose distribution	Dose [GyE]	diff. from the prescribed dose [%]	
CTV (D95%)	54,3 ± 0,7	97,3 ± 1,2	
Brainstem (D1cc)	52,9 ± 1,4	94,8 ± 2,6	
Brain (D1cc)	56,3 ± 0,5	100,9 ± 0,9	
1 LET Opt			
Brain: 4,6 keV/nm, 43GyE, 0,3% Brainstem: 2,5keV/nm, 50GyE, 5%			
Dose distribution	Dose [GyE]	diff. from the prescribed dose [%]	diff. from Clinical plan [%]
CTV (D95%)	53,7 ± 0,5	96,3 ± 1,0	-1,0 ± 0,7
Brainstem (D1cc)	49,8 ± 2,8	89,3 ± 5,0	-5,2 ± 5,0
Brain (D1cc)	56,4 ± 0,4	101,1 ± 0,7	0,3 ± 0,5
2 LET Opt			
Brain: 4,2 keV/nm, 43GyE, 0,3% Brainstem: 2keV/nm, 50GyE, 3,5%			

Dose distribution	Dose [GyE]	diff. from the prescribed dose [%]	diff. from Clinical plan [%]
CTV (D95%)	53,9 ± 0,4	96,6 ± 0,7	-1,4 ± 0,7
Brainstem (D1cc)	49,3 ± 2,9	88,3 ± 5,2	-7,0 ± 3,6
Brain (D1cc)	56,5 ± 0,3	101,3 ± 0,5	0,2 ± 0,4
3 LET Opt			
Brain: 3,8 keV/nm, 43GyE, 0,3% Brainstem: 1,5keV/nm, 50GyE, 2%			
Dose distribution	Dose [GyE]	diff. from the prescribed dose [%]	diff. from Clinical plan [%]
CTV (D95%)	53,5 ± 0,3	95,8 ± 0,8	-2,2 ± 1,1
Brainstem (D1cc)	48,6 ± 5,1	87,0 ± 5,6	-8,70 ± 4,8
Brain (D1cc)	56,6 ± 0,1	101,5 ± 0,8	0,4 ± 0,6
4 LET Opt			
Brain: 3,4 keV/nm, 43GyE, 0,3% Brainstem: 1keV/nm, 50GyE, 1%			
Dose distribution	Dose [GyE]	diff. from the prescribed dose [%]	diff. from Clinical plan [%]
CTV (D95%)	53,5 ± 0,3	95,8 ± 0,5	-2,0 ± 0,9
Brainstem (D1cc)	47,8 ± 5,1	85,6 ± 9,1	-8,6 ± 7,6
Brain (D1cc)	56,4 ± 0,1	101,1 ± 0,2	-0,01 ± 0,5
Gantry w/o LET Opt			
Brain: - Brainstem: -			
Dose distribution	Dose [GyE]	diff. from the prescribed dose [%]	diff. from Clinical plan [%]
CTV (D95%)	54,1 ± 0,5	96,9 ± 0,9	-0,3 ± 1,1
Brainstem (D1cc)	52,5 ± 1,6	94,0 ± 2,9	-0,8 ±1,7
Brain (D1cc)	56,4 ± 0,8	101,1 ± 1,4	0,3 ± 1,2
Gantry + LET Opt 1			
Brain: 3,8 keV/nm, 43GyE, 0,3% Brainstem: 2,5keV/nm, 50GyE, 5%			
Dose distribution	Dose [GyE]	diff. from the prescribed dose [%]	diff. from Clinical plan [%]
CTV (D95%)	54,0 ± 0,6	96,8 ± 1,1	-0,5 ± 1,3

Brainstem (D1cc)	51,6 ± 2,0	92,5 ± 3,6	-2,4 ± 3,0
Brain (D1cc)	56,6 ± 0,5	101,5 ± 1,0	0,6 ± 1,3
Gantry + LET Opt 2			
Brain: 3,4 keV/nm, 43GyE, 0,3% Brainstem: 2 keV/nm, 50GyE, 3,5%			
Dose distribution	Dose [GyE]	diff. from the prescribed dose [%]	diff. from Clinical plan [%]
CTV (D95%)	53,8 ± 0,6	96,5 ±1,1	-1,1 ± 1,3
Brainstem (D1cc)	50,6 ± 2,1	90,6 ± 3,8	-4,4 ± 3,5
Brain (D1cc)	56,6 ± 0,5	101,4 ± 1,0	0,6 ± 1,2
Gantry + LET Opt 3			
Brain: 3 keV/nm, 43GyE, 0,3% Brainstem: 1,5keV/nm, 50GyE, 2%			
Dose distribution	Dose [GyE]	diff. from the prescribed dose [%]	diff. from Clinical plan [%]
CTV (D95%)	53,3 ± 0,4	95,8 ± 0,6	-2,0 ± 1,1
Brainstem (D1cc)	47,3 ± 2,2	84,8 ± 3,9	-10,2 ± 3,6
Brain (D1cc)	56,6 ± 0,6	101,4 ± 1,1	0,3 ± 1,3
Gantry + LET Opt 4			
Brain: 2,6 keV/nm, 43GyE, 0,3% Brainstem: 1keV/nm, 50GyE, 1%			
Dose distribution	Dose [GyE]	diff. from the prescribed dose [%]	diff. from Clinical plan [%]
CTV (D95%)	53,3 ± 0,2	95,5 ± 0,4	-2,1 ± 0,9
Brainstem (D1cc)	46,2 ± 2,1	82,8 ± 3,7	-11,1 ± 3,6
Brain (D1cc)	56,7 ± 0,7	101,7 ±1,2	0,4 ± 1,9

Table 4. *Dose distribution for CTV (D95%) and for brain and brainstem structures (D1cc) across all planning approaches and for the clinical plan*

The results are visually summarized in ***Figures 15-16*** and ***17*** present the results of dose distribution for the clinical target volume (CTV) and organs at risk (OARs), specifically brain and brainstem structures, across all investigated planning approaches, including the Clinical plan, LET-optimized plans, and Gantry-based strategies. These results illustrate both the dose coverage of the target (CTV D95%) and the maximum dose received by critical structures (D1cc), as well as the relative deviation from the clinical dose baseline.

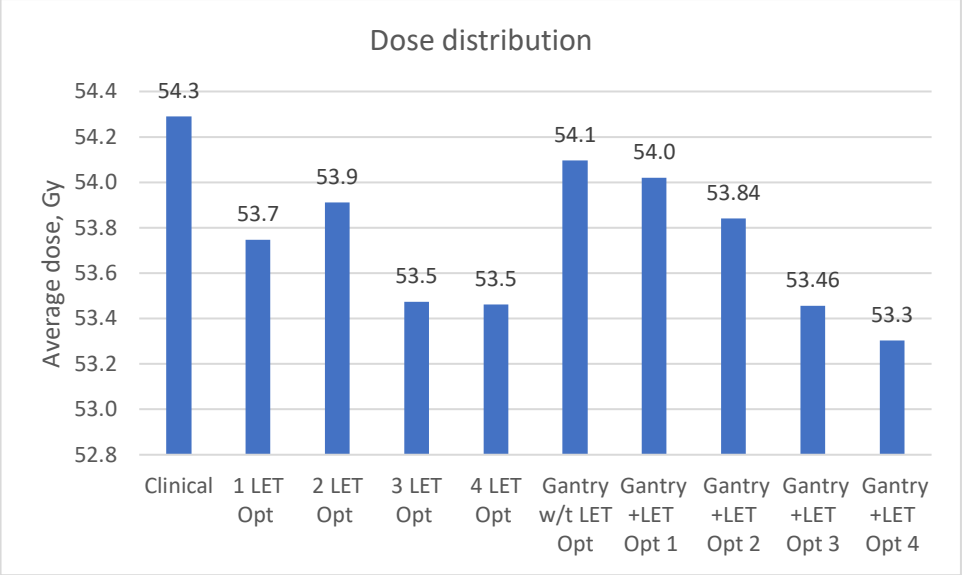

Figure 15. *Dose distribution for CTV (D95%) across all planning approaches and for the clinical plan*

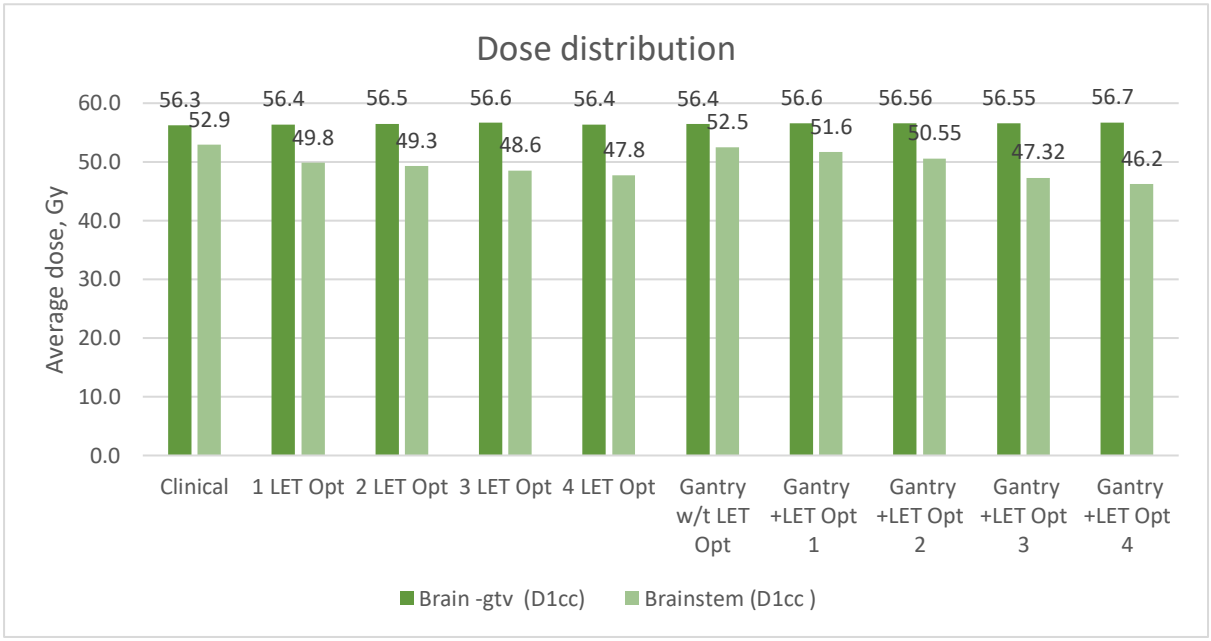

Figure 16. *Dose distribution for brain and brainstem structures (D1cc) across all planning approaches and for the clinical plan*

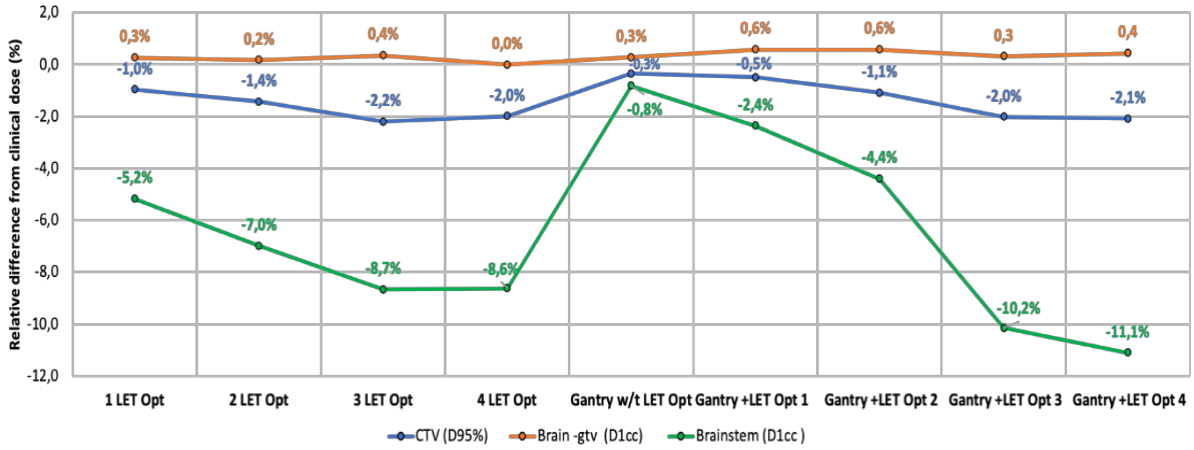

Figure 17. *Relative difference from the clinical dose (%) for CTV D95% and for brain and brainstem structures (D1cc) for all planning approaches and for the clinical plan*

As shown in ***Figures 18*** and ***19***, *CI* values across all approaches ranged between 0.90 and 0.95, and *HI* values varied from 0.89 to 0.97 depending on the plan. These results indicate an acceptable quality of target coverage and dose uniformity. According to ICRU Report 83, *CI* values between 0.9 and 1.1 and *HI* values up to 1.1–1.2 are considered clinically acceptable [24]. Based on these criteria, all evaluated planning strategies—regardless of LET optimization or gantry configuration—meet the standards for clinical applicability in terms of dose conformity and homogeneity.

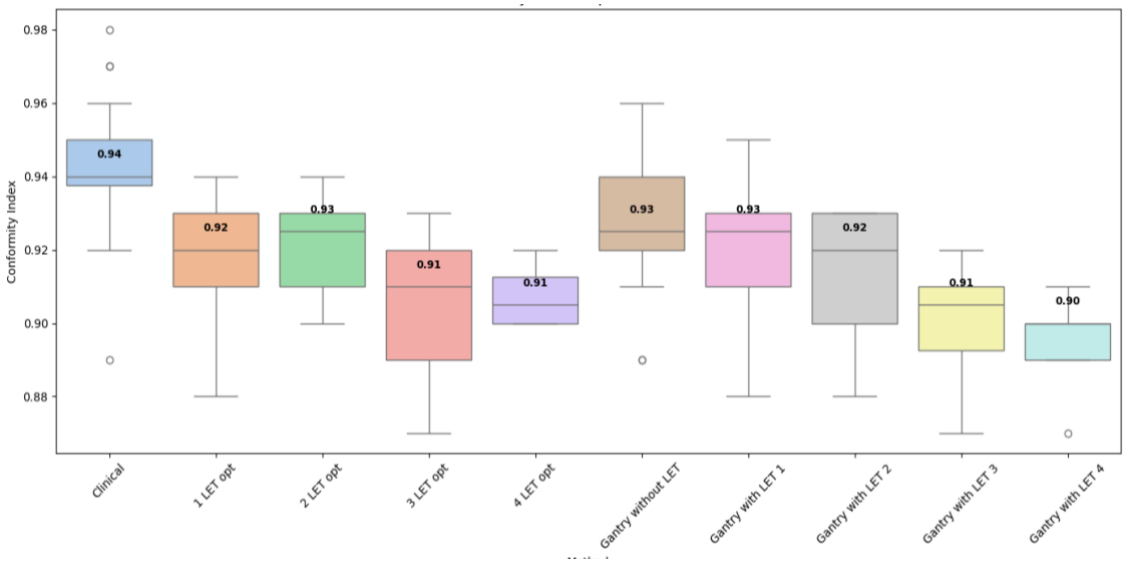

Figure 18. *Conformity Index (CI) comparison among all planning approaches, including Clinical, LET-optimized, and Gantry-based strategies*

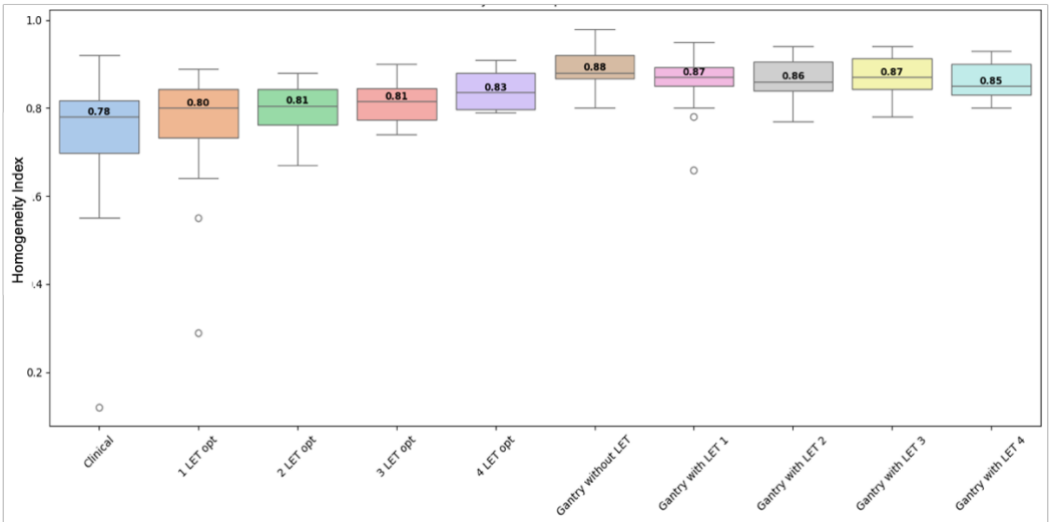

Figure 19. *Homogeneity Index (HI) comparison among all planning approaches, including Clinical, LET-optimized, and Gantry-based strategies*

The following ***Figure 20*** presents a comparison of the mean dose to the "Health Tissue – CTV" structure across all investigated planning approaches. As shown in the Figure, the use of gantry-based geometry leads to a reduction in the average dose to healthy tissues compared to approaches that rely solely on coplanar beams. For instance, the mean dose in the clinical plan was 2.83 GyE, while in gantry-based plans without LET optimization it decreased to 2.63 GyE. The highest mean dose was observed in the LET opt 4 approach, reaching 3.73 GyE, but this result may be influenced by the small sample size in that group, which included only four plans and therefore limits the statistical reliability of the finding.

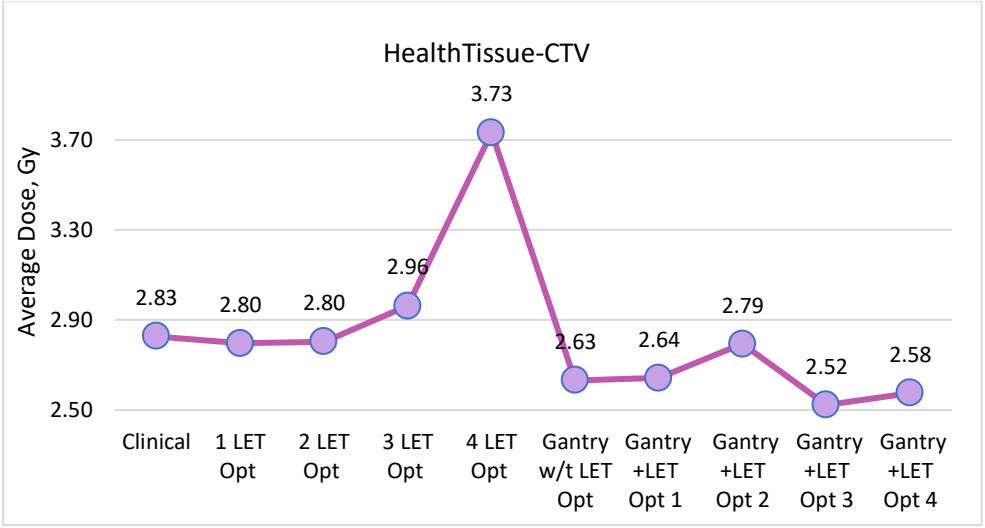

Figure 20. *Mean dose to the "Health Tissue-CTV" structure across all planning approaches*

2. LET distribution analysis

Clinical plans: In the Brain structure, the LETd value at 43 GyE and a volume of 1 cm^3 was 5.1 keV/µm ± 0,4 keV/µm, exceeding the 4.6 keV/µm threshold linked to a higher risk of necrosis. These constraints were informed by the findings of Bazani A. et al., who reported a correlation between necrosis and three key factors: dose levels above 42.9 GyE, small irradiated volumes (<5 cm^3, ideally <1 cm^3), and elevated LETd values (4.6 keV/µm) [34].

Based on these data—specifically, the brain volume receiving more than 42.9 GyE and the presence or absence of Grade 1 radionecrosis—an NTCP (Normal Tissue Complication Probability) curve was constructed.

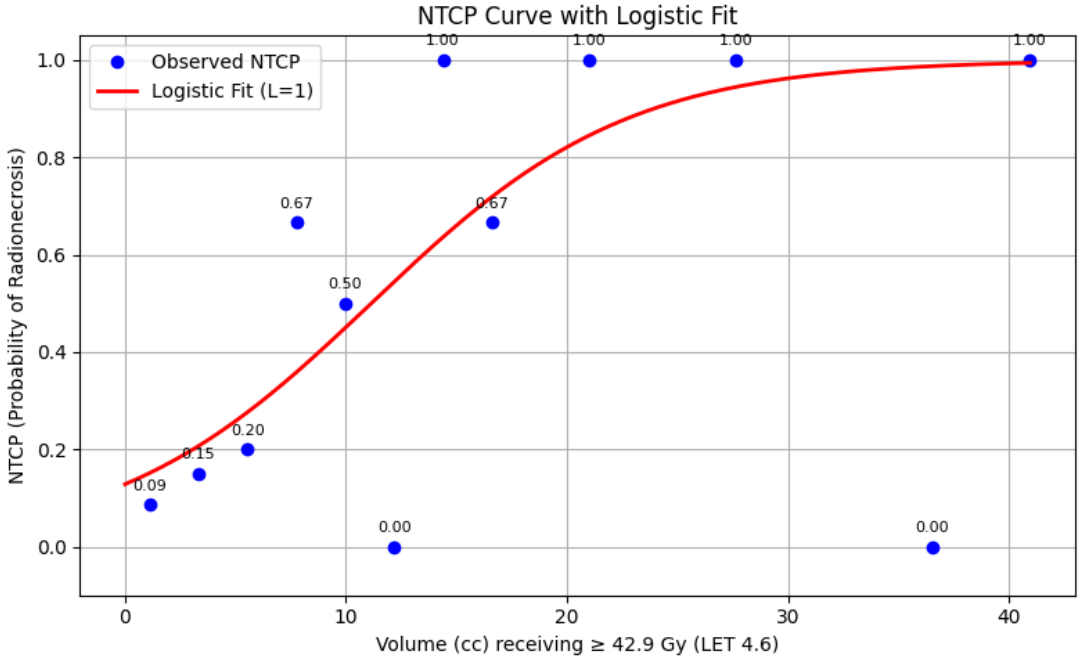

Figure 21. *NTCP curve reflecting the probability of G1 brain necrosis at dose >42.9 GyE, LET>4.6 keV/µm and volume <5 cm^3*

The NTCP curve represents a model that quantitatively estimates the probability of complications developing in healthy tissues during radiation therapy, based on dose and LET parameters. Its primary purpose is to predict the risk of damage to critical structures and to support clinically informed decision-making in treatment planning, aiming to achieve an optimal balance between therapeutic efficacy and patient safety.

For the brainstem, the LET at a dose of 50 GyE and a volume of 1 cm^3 was 3.5 keV/µm ± 0,4 keV/µm**.** However, since optimization is expected to reduce the volume receiving high LET, an additional analysis was performed for a smaller volume of 0.5 cm^3, where the LET was 3.9 keV/µm ± 0,5 keV/µm**.**

After LETd optimization «1 LET Opt»: LETd values in the brain decreased from 5.1 ± 0,4 keV/µm to 4.5 keV/µm ± 0,1 keV/µm, and in the brainstem from 3.5 ± 0,4 keV/µm to 2.3 keV/µm ± 0,8 keV/µm.

The results of the subsequent LETd-optimized plans (2–4 LET opt), LETd-optimized plans with gantry-based beam geometry (Gantry+LET opt 1–4), and plans without LETd optimization but with gantry-based geometry (Gantry w/o LET opt) are presented in ***Table 5***.

Clinical plans		
LET	LET [keV/µm]	
LET Brain 1cc	5,1 ± 0,4	
LET Brainstem1cc	3,5 ± 0,4	
LET Brainstem 0,5cc	3,9 ± 0,5	
1 LET Opt		
Brain: 4,6 keV/nm, 43GyE, 0,3% Brainstem: 2,5keV/nm, 50GyE, 5%		
LET	LET [keV/µm]	diff. from Clinical plan [keV/µm]
LET Brain 1cc	4,5 ± 0,1	0,6 ± 0,4
LET Brainstem1cc	2,3 ± 0,8	1,2 ± 0,9
LET Brainstem 0,5cc	2,9 ± 0,5	1,0 ± 0,5
2 LET Opt		
Brain: 4,2 keV/nm, 43GyE, 0,3% Brainstem: 2keV/nm, 50GyE, 3,5%		
LET	LET [keV/µm]	diff. from Clinical plan [keV/µm]
LET Brain 1cc	4,3 ± 0,2	0,9 ± 0,5
LET Brainstem1cc	2,0 ± 1,1	1,6 ±1,1
LET Brainstem 0,5cc	2,7 ± 1,1	1,2 ± 1,1
3 LET Opt		
Brain: 3,8 keV/nm, 43GyE, 0,3% Brainstem: 1,5keV/nm, 50GyE, 2%		
LET	LET [keV/µm]	diff. from Clinical plan [keV/µm]
LET Brain 1cc	3,9 ± 0,3	1,2 ± 0,5

LET Brainstem1cc	2,1 ± 1,1	2,3 ± 1,4
LET Brainstem 0,5cc	2,3 ± 0,9	1,6 ± 1,1
4 LET Opt		
Brain: 3,4 keV/nm, 43GyE, 0,3% Brainstem: 1keV/nm, 50GyE, 1%		
LET	LET [keV/µm]	diff. from Clinical plan [keV/µm]
LET Brain 1cc	3,5 ± 0,2	1,5 ± 0,3
LET Brainstem1cc	1,3 ± 1,5	2,0 ± 1,7
LET Brainstem 0,5cc	2,0 ± 1,4	1,7 ± 1,8
Gantry w/o LET Opt		
Brain: - Brainstem: -		
LET	LET [keV/µm]	diff. from Clinical plan [keV/µm]
LET Brain 1cc	4,2 ± 0,6	0,9 ± 0,5
LET Brainstem1cc	3,0 ± 0,5	0,5 ± 0,6
LET Brainstem 0,5cc	3,3 ± 0,6	0,6 ± 0,7
Gantry + LET Opt 1		
Brain: 3,8 keV/nm, 43GyE, 0,3% Brainstem: 2,5keV/nm, 50GyE, 5%		
LET	LET [keV/µm]	diff. from Clinical plan [keV/µm]
LET Brain 1cc	3,8 ± 0,2	1,3 ± 0,4
LET Brainstem1cc	2,4 ± 0,3	1,1 ± 0,5
LET Brainstem 0,5cc	2,7 ± 0,3	1,2 ± 0,7
Gantry + LET Opt 2		
Brain: 3,4 keV/nm, 43GyE, 0,3% Brainstem: 2 keV/nm, 50GyE, 3,5%		
LET	LET [keV/µm]	diff. from Clinical plan [keV/µm]
LET Brain 1cc	3,5 ± 0,2	1,6 ± 0,4
LET Brainstem1cc	2,1 ± 0,4	1,5 ± 0,7
LET Brainstem 0,5cc	2,4 ± 0,5	1,6 ± 0,9
Gantry + LET Opt 3		
Brain: 3 keV/nm, 43GyE, 0,3% Brainstem: 1,5keV/nm, 50GyE, 2%		
LET	LET [keV/µm]	diff. from Clinical plan [keV/µm]
LET Brain 1cc	3,2 ± 0,2	2,0 ± 0,5
LET Brainstem1cc	1,3 ± 1,1	2,3 ±1,5

LET Brainstem 0,5cc	2,1 ± 0,8	1,8 ± 1,2
Gantry + LET Opt 4		
Brain: 2,6 keV/nm, 43GyE, 0,3% Brainstem: 1keV/nm, 50GyE, 1%		
LET	LET [keV/µm]	diff. from Clinical plan [keV/µm]
LET Brain 1cc	2,9 ± 0,4	2,1 ± 0,5
LET Brainstem1cc	1,5 ± 1,2	2,6 ± 1,6
LET Brainstem 0,5cc	1,7 ± 1,0	2,2 ± 1,5

Table 5. *LET distribution for brain (1cc) and brainstem structures (1cc and 0,5cc) across all planning approaches and for the Clinical plan*

Figure 22 provide an analysis of LET distributions for different planning approaches. These results highlight how the optimization strategy and beam geometry influence the spatial distribution and magnitude of LET in critical structures such as the brain and brainstem.

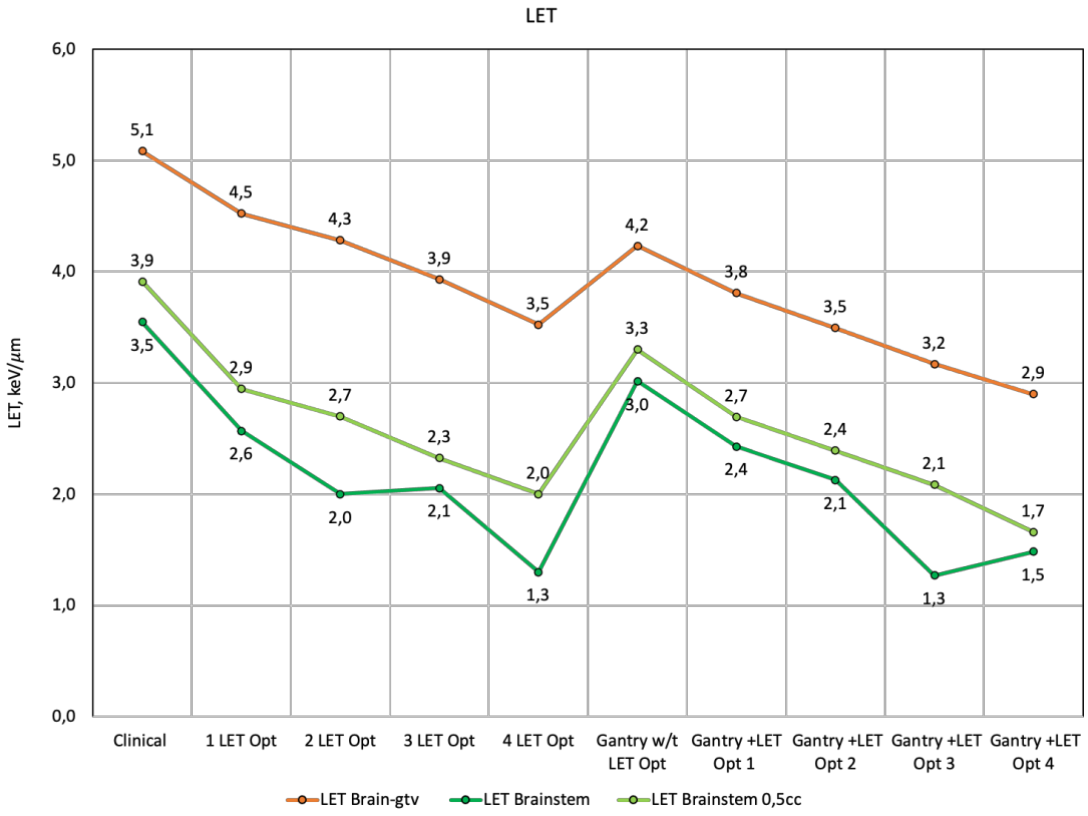

Figure 22. *LETd values for the brain structure at 43 GyE and 1 cm³, and for the brainstem structure at 50 GyE with volumes of 1 cm³ and 0.5 cm³, across all planning approaches and the clinical plan*

3. Robustness analysis

Clinical plans: For the clinical target volume (CTV), the condition D95% = V95% was met in 83.9% of scenarios, which corresponds to 94.8% of the prescribed dose. However, the stricter criterion D98% = V98% was achieved in only 0.4% of scenarios, indicating a high sensitivity of minimum coverage to uncertainties.

The constraint reflecting the presence of "hotspots" (D103% = V1%) was fulfilled in 62.4% of cases, with the maximum dose in the worst-case scenario reaching 58.6 GyE ± 1,6 GyE, equivalent to 104,9% ± 2,9% of the prescribed dose, indicating moderate robustness in terms of local overdosing.

For the considered critical structures, robustness was demonstrated as 92.8% of scenarios met the Brain constraint (D103% ≤ V1cc), and 98.6% met the brainstem constraint (D100% ≤ V1cc). In the worst-case scenarios, the doses to the Brain and brainstem were 57.4 GyE ± 1,5 GyE and 54.8 GyE ± 0,9 GyE, respectively.

After LETd optimization «1 LET Opt»: Inspecting the worst-case scenarios we observed that CTV D95 decreased by 2.4%, and CTV D98 by 3.9%. Meanwhile, CTV D1% increased by 1.3%. Evaluation of hot spots (D1cc) in the OARs showed a 0.4% dose increase in the brain and a 2.2% decrease in the brainstem.

The results of the subsequent LETd-optimized plans (2–4 LET opt), LETd-optimized plans with gantry-based beam geometry (Gantry + LET opt 1–4), and plans without LETd optimization but with gantry-based geometry (Gantry w/o LET opt) are presented in ***Table 6***.

Clinical plans			
Robust Evaluation	Passed [%]	worst scenario dose [GyE]	Worst scenario dose [% of prescribed]
CTV (D95%=V95%)	83,9 ± 21,8	52,9 ± 1,1	94,7 ± 1,9
CTV (D98%=V98%)	0,4 ± 1,8	51,2 ± 2,5	91,7 ± 4,4
CTV (D103%=1V%)	62,4 ± 33,8	58,6 ± 1,6	104,9± 2,9

Brain (D103%=V1cc)	92,8 ± 15,2	57,4 ± 1,5	102,9± 2,7	
Brainstem (D100%=V1cc)	98,6 ± 5,6	54,8 ± 0,9	98,3± 1,6	
1 LET Opt				
Brain: 4,6 keV/nm, 43GyE, 0,3% Brainstem: 2,5keV/nm, 50GyE, 5%				
Robust Evaluation	Passed [%]	worst scenario dose [GyE]	Worst scenario dose [% of prescribed]	diff. from Clinical plan [%]
CTV (D95%=V95%)	56,8 ± 23,8	51,6 ± 1,1	92,5 ± 1,9	-2,4 ± 2,0
CTV (D98%=V98%)	0,0 ± 0,0	49,1 ± 2,2	88,0 ± 4,0	-3,9 ± 2,7
CTV (D103%=1V%)	46,4 ±2 9,3	59,2 ± 1,4	106,1 ± 2,6	1,3 ± 1,6
Brain (D103%=V1cc)	88,8 ± 14,1	57,6 ± 1,0	103,2 ± 1,7	0,4 ± 1,5
Brainstem (D100%=V1cc)	100,0 ± 0,0	53,2 ± 1,7	95,3 ± 3,0	-2,2 ± 3,7
2 LET Opt				
Brain: 4,2 keV/nm, 43GyE, 0,3% Brainstem: 2keV/nm, 50GyE, 3,5%				
Robust Evaluation	Passed [%]	worst scenario dose [GyE]	Worst scenario dose [% of prescribed]	diff. from Clinical plan, [%]
CTV (D95%=V95%)	54,3 ± 20,0	51,4 ± 1,0	92,1 ± 1,8	-3,3 ± 1,8
CTV (D98%=V98%)	0,0 ± 0,0	48,8 ± 1,2	87,5 ± 2,1	-5,8 ± 2,8
CTV (D103%=1V%)	29,9 ± 26,6	60,2 ± 1,2	107,9 ± 2,2	2,0 ± 2,0
Brain (D103%=V1cc)	88,6 ± 13,5	58,0 ± 1,0	103,9 ± 1,7	0,7 ± 2,1
Brainstem (D100%=V1cc)	99,7 ± 1,2	52,7 ± 2,0	94,4 ± 3,5	-4,5 ± 3,9
3 LET Opt				
Brain: 3,8 keV/nm, 43GyE, 0,3% Brainstem: 1,5keV/nm, 50GyE, 2%				
Robust Evaluation	Passed [%]	worst scenario dose [GyE]	Worst scenario dose [% of prescribed]	diff. from Clinical plan [%]
CTV (D95%=V95%)	34,2 ± 23,3	50,8 ± 1,0	91,0 ± 1,7	-4,3 ± 2,3
CTV (D98%=V98%)	0,0 ± 0,0	47,7 ±1,8	85,6 ± 3,3	-7,8 ± 3,7

CTV (D103%=1V%)	24,6 ± 27,3	60,2 ± 1,3	107,8 ± 2,3	1,7 ± 1,9
Brain (D103%=V1cc)	83,8 ± 16,4	57,3 ± 1,9	102,8 ± 3,5	-0,6 ± 2,8
Brainstem (D100%=V1cc)	99,6 ± 1,3	52,0 ± 2,3	93,2 ± 4,1	-6,1 ± 4,7
4 LET Opt				
Brain: 3,4 keV/nm, 43GyE, 0,3% Brainstem: 1keV/nm, 50GyE, 1%				
Robust Evaluation	Passed [%]	worst scenario dose [GyE]	Worst scenario dose [% of prescribed]	diff. from Clinical plan [%]
CTV (D95%=V95%)	31,3 ± 16,1	50,5 ± 0,7	90,5 ± 1,3	-3,9 ± 3,4
CTV (D98%=V98%)	0,0 ± 0,0	47,5 ± 0,6	85,1 ± 1,1	-7,3 ± 4,2
CTV (D103%=1V%)	24,0 ± 18,2	60,4 ± 1,3	108,2 ± 2,4	2,2 ± 2,8
Brain (D103%=V1cc)	89,8 ± 15,6	57,7 ± 0,8	103,4 ± 1,5	-0,9 ± 2,6
Brainstem (D100%=V1cc)	100,0 ± 0,0	51,9 ± 3,6	93,0 ± 6,5	-5,8 ± 7,2
Gantry w/o LET Opt				
Brain: - Brainstem: -				
Robust Evaluation	Passed [%]	worst scenario dose [GyE]	Worst scenario dose [% of prescribed]	diff. from Clinical plan [%]
CTV (D95%=V95%)	57,3 ± 30,2	51,7 ± 2,8	92,6 ± 4,9	-2,3 ± 4,3
CTV (D98%=V98%)	0,0 ± 0,0	50,3 ± 1,8	90,1 ± 3,3	-1,7 ± 3,6
CTV (D103%=1V%)	24,8 ± 34,8	59,5 ± 1,3	106,6 ± 2,3	1,6 ± 2,1
Brain (D103%=V1cc)	81,5 ± 25,3	57,7 ± 1,3	103,4 ± 2,4	0,5 ± 1,8
Brainstem (D100%=V1cc)	98,8 ± 3,2	54,7 ± 1,2	98,0 ± 2,2	-0,2 ± 1,9
Gantry + LET Opt 1				
Brain: 3,8 keV/nm, 43GyE, 0,3% Brainstem: 2,5keV/nm, 50GyE, 5%				
Robust Evaluation	Passed [%]	worst scenario dose [GyE]	Worst scenario dose [% of prescribed]	diff. from Clinical plan [%]
CTV (D95%=V95%)	56,1 ± 32,8	52,0 ± 1,1	93,1 ± 1,9	-1,7 ± 2,2

CTV (D98%=V98%)	0,0 ± 0,0	50,0 ± 1,8	89,5 ± 3,3	-2,3 ± 3,8
CTV (D103%=1V%)	16,5 ± 27,3	59,8 ± 1,1	107,2 ± 2,0	2,2 ± 2,6
Brain (D103%=V1cc)	77,6 ±25,8	57,9 ± 0,8	103,8 ± 1,4	0,8 ± 2,0
Brainstem (D100%=V1cc)	97,6 ± 6,9	54,9 ± 1,8	98,4 ± 3,2	0,2 ± 3,5
Gantry + LET Opt 2				
Brain: 3,4 keV/nm, 43GyE, 0,3% Brainstem: 2 keV/nm, 50GyE, 3,5%				
Robust Evaluation	Passed [%]	worst scenario dose [Gy]	Worst scenario dose [% of prescribed]	diff. from Clinical plan [%]
CTV (D95%=V95%)	40,4 ± 33,5	51,4 ± 1,1	92,1 ±2,0	-3,0 ± 2,9
CTV (D98%=V98%)	0,0 ± 0,0	49,3 ± 1,2	88,3 ±2,2	-4,5 ± 3,7
CTV (D103%=1V%)	12,7 ± 23,2	60,1 ± 1,1	107,7 ± 1,9	2,7 ± 3,1
Brain (D103%=V1cc)	81,8 ± 20,8	57,9 ± 0,8	103,7 ± 1,4	1,1 ± 2,2
Brainstem (D100%=V1cc)	97,0 ± 5,7	54,7 ± 2,0	98,1 ± 3,6	-0,3 ± 4,0
Gantry + LET Opt 3				
Brain: 3 keV/nm, 43GyE, 0,3% Brainstem: 1,5keV/nm, 50GyE, 2%				
Robust Evaluation	Passed [%]	worst scenario dose [GyE]	Worst scenario dose [% of prescribed]	diff. from Clinical plan [%]
CTV (D95%=V95%)	22,0 ± 19,3	50,9 ± 0,9	91,1 ± 1,5	-3,8 ± 2,7
CTV (D98%=V98%)	0,0 ± 0,0	48,5 ± 1,1	86,8 ±2,0	-5,6 ± 3,8
CTV (D103%=1V%)	11,7 ± 22,4	60,1 ± 1,3	107,7 ± 2,2	1,9 ± 3,0
Brain (D103%=V1cc)	83,0 ± 23,2	57,7 ± 0,7	103,3 ± 1,3	0,1 ± 2,8
Brainstem (D100%=V1cc)	100,0 ± 0,0	51,8 ± 2,0	92,8 ± 3,6	-6,0 ± 3,6
Gantry + LET Opt 4				
Brain: 2,6 keV/nm, 43GyE, 0,3% Brainstem: 1keV/nm, 50GyE, 1%				
Robust Evaluation	Passed [%]	worst scenario dose [GyE]	Worst scenario dose [% of prescribed]	diff. from Clinical plan [%]

CTV (D95%=V95%)	18,2 ± 11,3	50,3 ± 0,4	90,1 ± 0,7	-3,5 ± 3,0
CTV (D98%=V98%)	0,0 ± 0,0	47,9 ± 0,5	85,8 ± 1,0	-4,8 ± 3,9
CTV (D103%=1V%)	1,6 ± 3,6	61,3 ± 1,7	109,8 ± 3,1	2,5 ± 4,9
Brain (D103%=V1cc)	76,0 ± 24,4	58,3 ± 0,9	104,5 ± 1,7	0,8 ± 4,8
Brainstem (D100%=V1cc)	100,0 ± 0,0	51,0 ± 2,3	91,3 ±4,1	-7,7 ± 4,7

Table 6. *Results of the robust evaluation of dose metrics for CTV (D95%, D98%, and D1%) and for brain and brainstem (D1cc) across all planning approaches and for the Clinical plan*

Figures 23–26 summarize the dosimetric variations observed in the worst-case scenario. ***Figures 23*** and ***24*** show the results for target coverage metrics (CTV D95%, D98%, and D1%) and the evaluation of potential hot spots in critical structures (D1cc for the brain and brainstem). ***Figures 25*** and ***26*** present results that enable a comparative assessment of the robustness of each planning approach relative to the clinical plan.

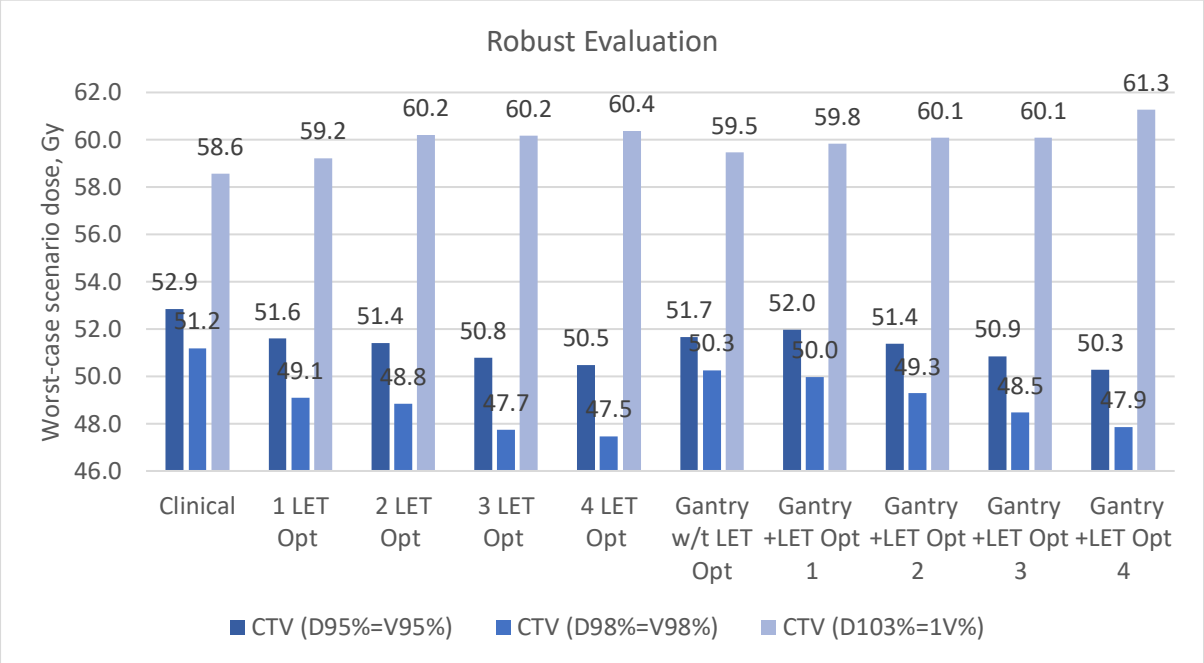

Figure 23. *Dose values in the worst-case scenario for CTV D95%, CTV D98%, CTV D1%, across all planning approaches and the clinical plan*

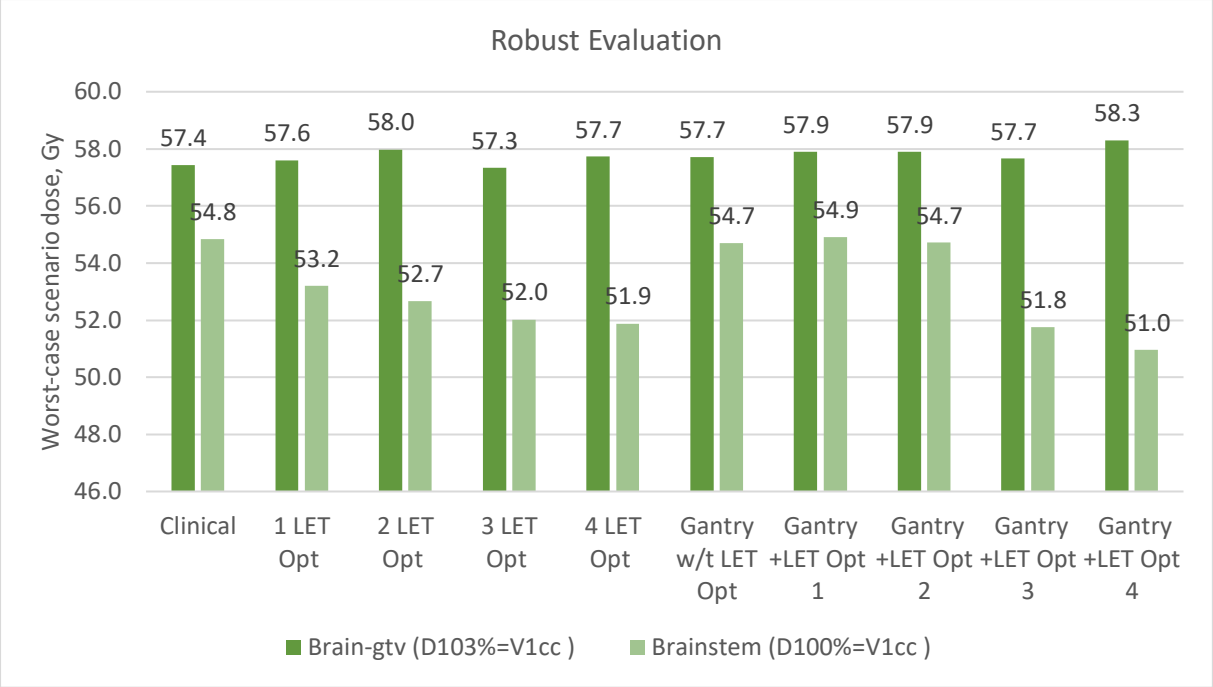

Figure 24. *Dose values in the worst-case scenario for the brain (D1cc) and brainstem (D1cc) across all planning approaches and the clinical plan*

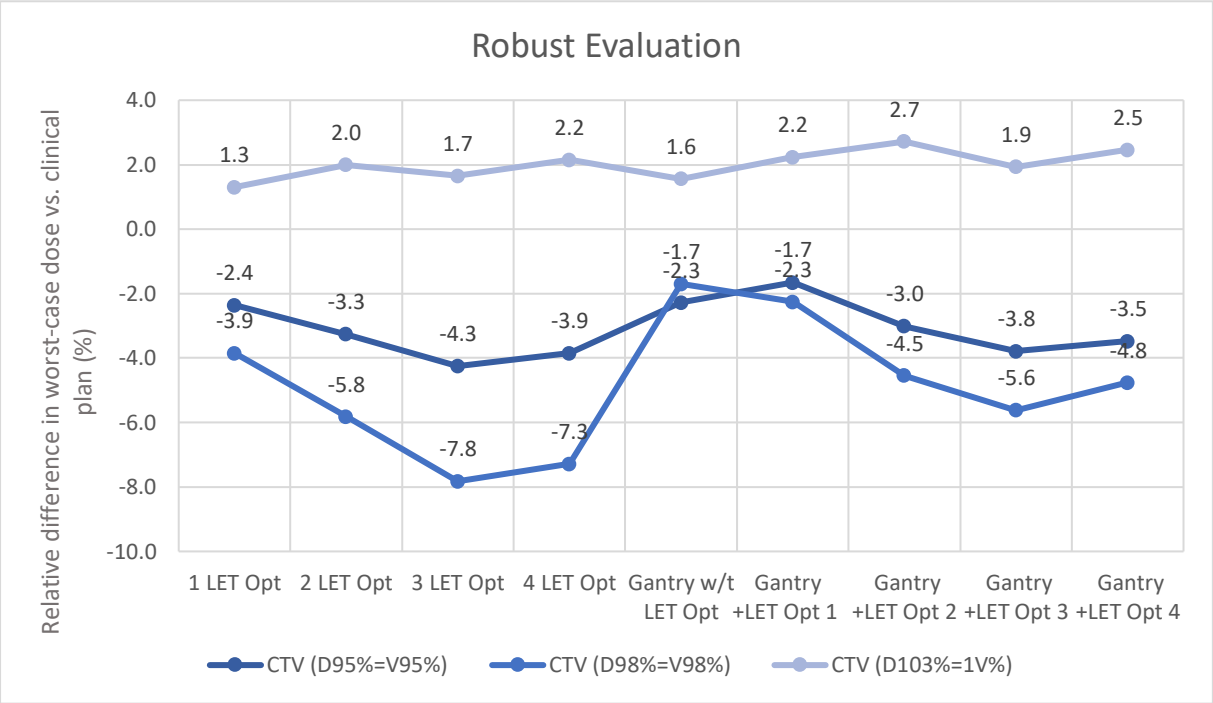

Figure 25. *Relative dose difference in the worst-case scenario for CTV D95%, CTV D98%, CTV D1% compared to the clinical plan*

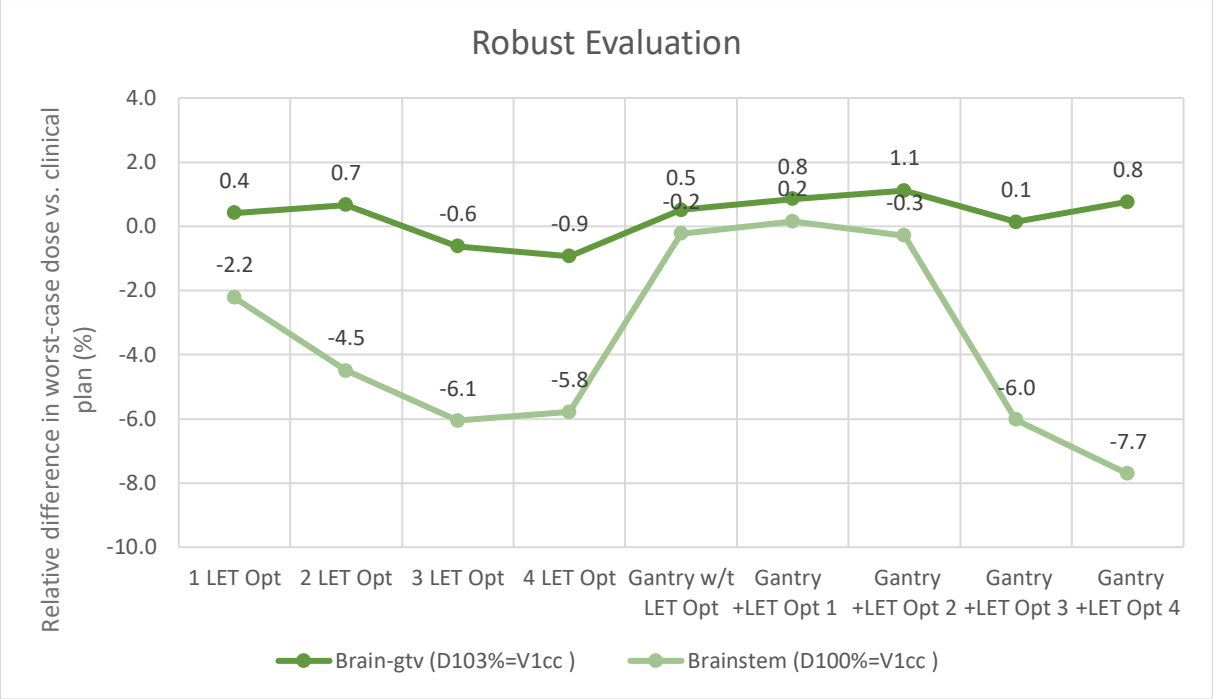

Figure 26. *Relative dose difference in the worst-case scenario for the brain (D1cc) and brainstem (D1cc), compared to the clinical plan*

Discussion

In this study, we analyzed the potential clinical impact of integrating LET optimization into the treatment planning workflow for proton therapy of brain tumors. Recent advances in commercial TPS allow not only for the visualization but also the optimization of LET distributions during dose optimization. However, despite the well-established importance of LET optimization in the literature, there remains limited consensus on reference LET values (e.g., LET at specific dose levels) to guide clinical decision-making.

In the first part of the study, we implemented a normal tissue complication probability (NTCP) model as a function of LETd values, based on a retrospective clinical cohort of brain tumor patients treated at CNAO and followed up over time [34].

Subsequently, a cohort of 20 brain tumor patients with similar morphological and dosimetric characteristics was selected. For each patient, a clinical proton therapy plan previously generated at CNAO was available. These plans were re-optimized multiple times using various LET optimization strategies aimed at improving LET distributions while maintaining acceptable dose distribution quality. The optimization procedures were performed for both fixed-beam and gantry-based geometries.

The resulting plans were comprehensively analyzed with respect to three key aspects: dose distribution quality, LETd maps, and robustness against clinically relevant uncertainties. This enabled the identification of the best achievable trade-offs among these competing factors within the framework of a realistic clinical planning workflow for brain tumors.

Finally, the potential reduction in the risk of radiation-induced side effects in healthy tissue was estimated for the newly optimized plans, based on the previously developed NTCP model.

The following section presents the spatial distributions of dose and LETd for the clinical plan and the comparative approaches, providing a visual representation of the effects of different planning strategies. The following ***Figure 27*** shows the dose distributions for the Clinical Plan (Clinical), the LET-optimized plan (LET opt 3), the gantry-based plan without LET optimization (Gantry w/o LET), and the gantry-based plan with LET optimization (Gantry + LET opt 3). From the distributions, it can be observed that low-dose regions (highlighted with yellow arrows,

corresponding to 25% of the prescribed dose) are more prominent in the «Clinical» and «LET opt 3» plans compared to the gantry-based plans. This indicates that gantry-based plans allow for greater flexibility in beam arrangement, resulting in a more compact dose distribution. These observations are consistent with the previously reported lower mean dose in healthy tissues.

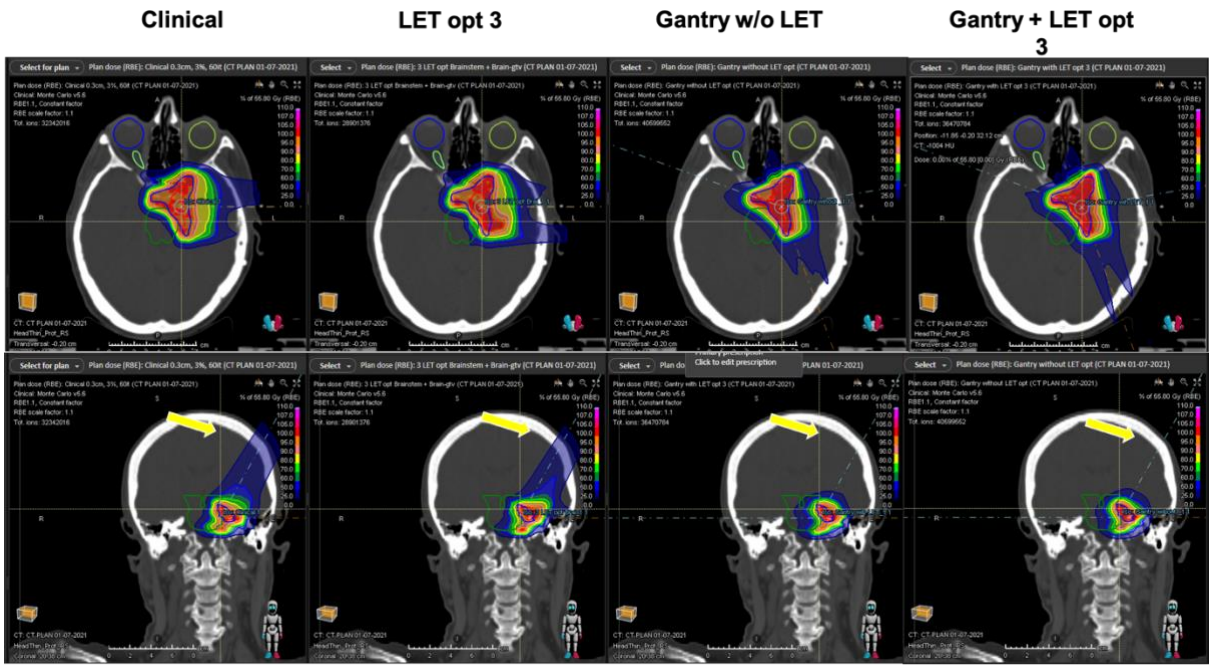

Figure 27. *Dose distribution for the Clinical Plan, «LET opt 3», «Gantry w/o LET», and «Gantry with LET opt 3»*

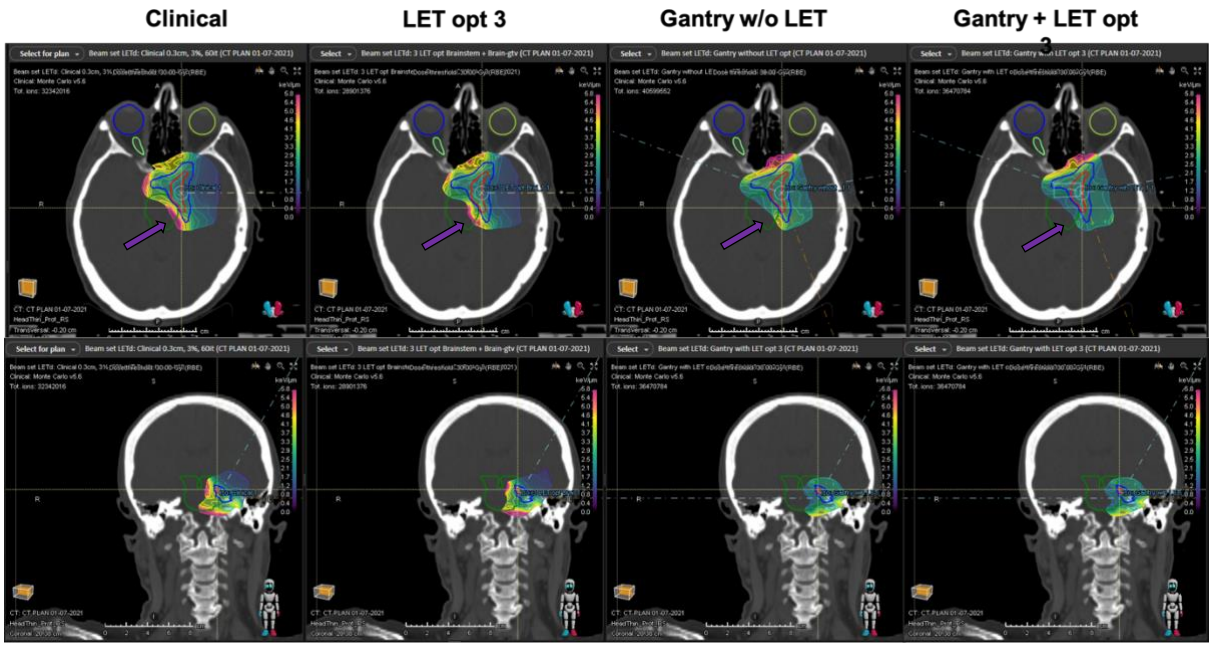

Figure 28. *LET distribution for the Clinical Plan, «LET opt 3», «Gantry w/o LET», and «Gantry with LET opt 3»*

Figure 28 shows the LET distributions for the same four planning strategies. From these distributions, it is evident that the «Clinical» and «LET opt 3» plans result in high LETd values within the brainstem, as indicated by the red regions (highlighted with violet arrows, corresponding to LETd≥5 keV/µm). In contrast, such elevated LETd values are not observed in the «Gantry w/o LET» and «Gantry + LET opt 3» plans, demonstrating effective LET optimization.

Figures 29–30 present the LET–Volume Histograms (LVHs) for the brain and brainstem structures, respectively. The same four planning strategies were compared, and the LVH script was used to extract LETd values at a dose of 2 GyE and a volume of 1 cm^3 to determine the maximum LETd within the structures. The histograms show that the «Clinical» plan exhibits the highest LETd values, as it was not optimized for LET. In the "LET opt 3" plan, the LETd is reduced by 0.8 keV/µm for the brain and 1.1 keV/µm for the brainstem. In the «Gantry w/o LET» plan, despite the absence of LET optimization, the LETd values are further reduced—by 1.9 keV/µm for the brain and 1.8 keV/µm for the brainstem—indicating the impact of beam arrangement. Finally, the «Gantry with LET opt 3» approach achieves the most substantial reduction in LETd values: 2.3 keV/µm for the brain and 2.2 keV/µm for the brainstem.

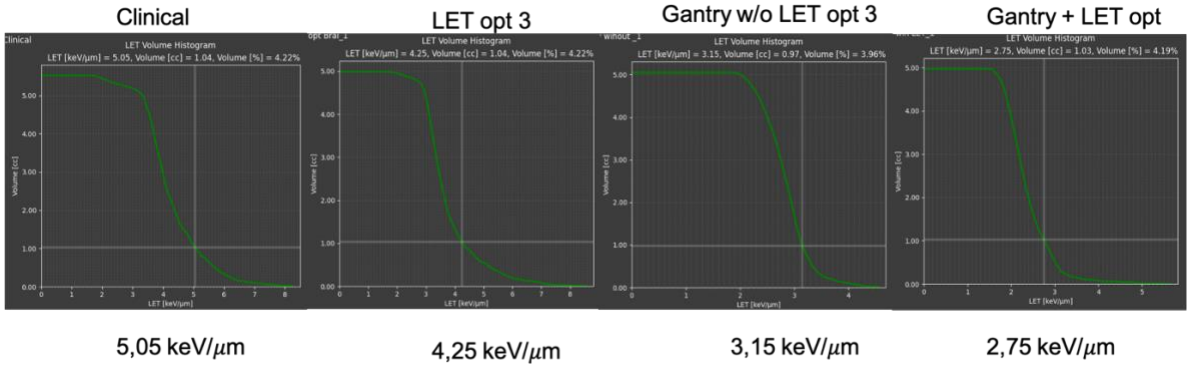

Figure 29. *LVHs for the brain structure in the Clinical Plan, «LET opt 3», «Gantry w/o LET», and «Gantry with LET opt 3»*

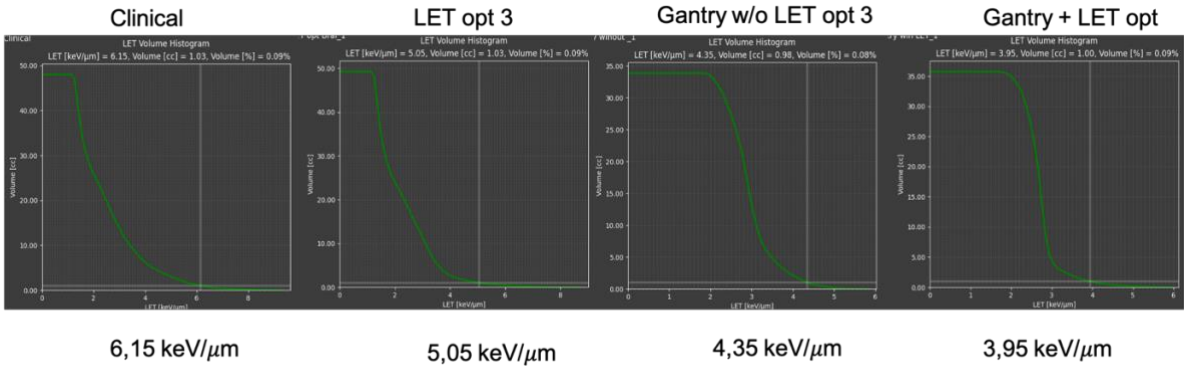

Figure 30. *LVHs for the brainstem structure in the Clinical Plan, «LET opt 3», «Gantry w/o LET», and «Gantry with LET opt 3»*

One of the key objectives of this study is to determine the trade-off between reducing LET levels in healthy tissues and maintaining acceptable plan quality in terms of dose coverage and robustness. As previously discussed, CTV coverage in optimized plans should remain clinically acceptable, i.e., no less than 95% of the prescribed dose. Regarding LET in organs at risk, it is preferable to reduce it below established threshold values, as exceeding these levels may be associated with increased risks of radionecrosis and other tissue damage. In terms of robustness analysis, a clinically acceptable deviation is defined as a dose variation within ±5% in the worst-case scenario compared to the clinical plan.

In ***Figure 31*** we presented the average value of LETd and target dose displacement for the considered patient cohort for the optimized plans – with or without a gantry geometry – when applying a different constraint on the brain structure for the brain structure. As LETd constraints become stricter, a consistent reduction in LETd is observed, confirming the effectiveness of optimization in terms of reducing the risk of radiation-induced damage. Simultaneously, a detriment in robustness is also noted: the stricter the constraints, the lower the maximum dose in the analyzed structure, which is generally considered a favorable outcome. However, the relationship between LETd and robustness in our study is not so clear. For instance, in the “Gantry with LET opt 4” approach, an increase in the maximum dose to the brain in the worst-case scenario is observed, despite achieving the lowest LETd value. This result may be attributed to the overly stringent constraints applied (2.6 keV/μm, 43 Gy, 0.3% volume), which likely forced the treatment planning system to compensate for the loss in CTV coverage by introducing localized hot spots at the interface between the target volume and

the brain. Indeed the best achievable option is “LET opt” for a fixed beam geometry, while is “Gantry +LET opt 4” for gantry, when reducing local LETd values at the brain.

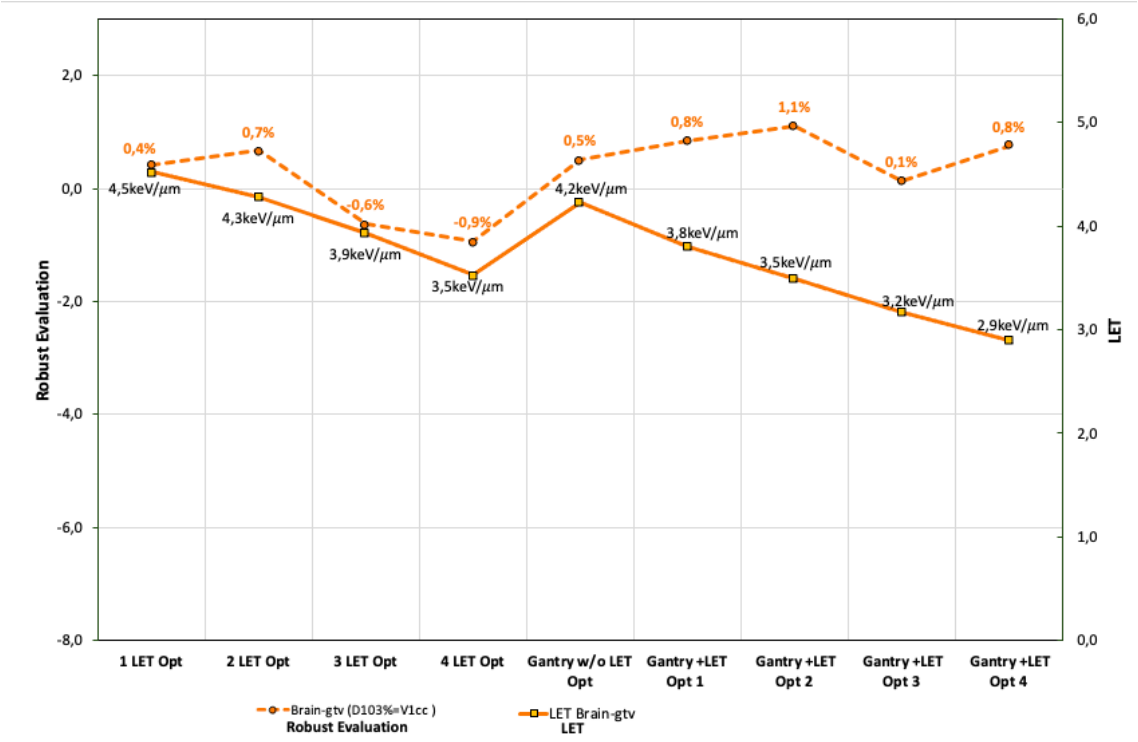

Figure 31. *Relationship Between LETd Values and Robustness Across Different Optimization Strategies for the Brain*

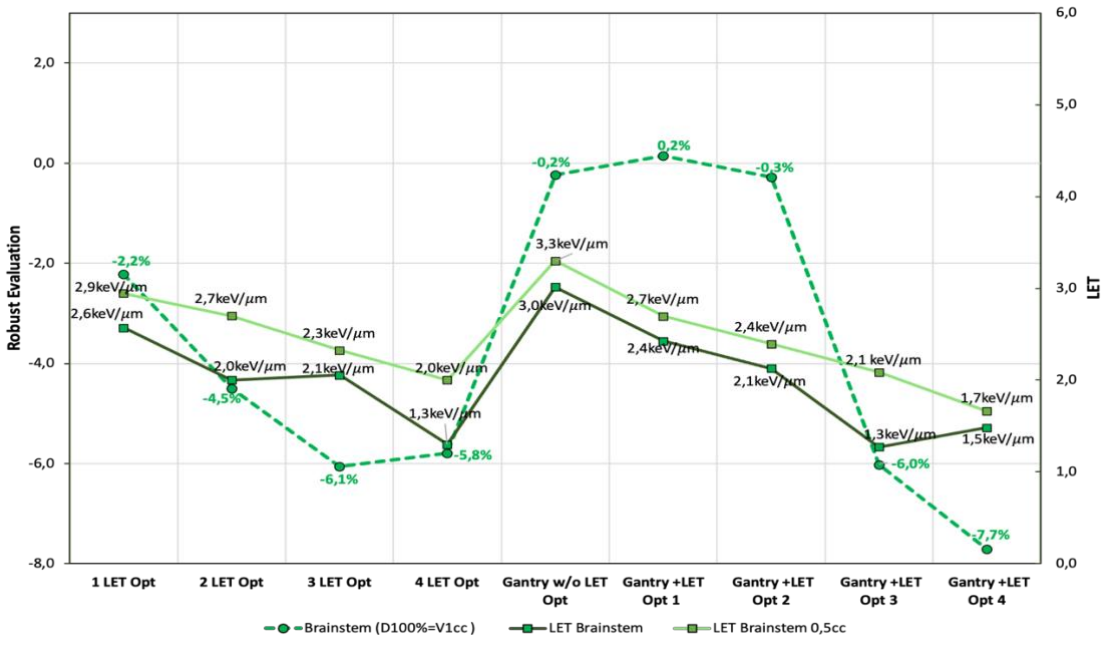

Figure 32. *Relationship Between LETd Values and Robustness Across Different Optimization Strategies for Brainstem*

Figure 32 presents data illustrating the relationship between LET levels and robustness (i.e., dose distribution reliability) for the brainstem across various planning approaches. The results reveal a general trend: as LET constraints become more stringent, both the LETd values and robustness metrics tend to decrease. For the “LET opt 3–4” and “Gantry with LET opt 3–4” approaches, robustness values exceed the acceptable threshold of ±5%. However, from a clinical perspective, this may be considered a favorable outcome, as a reduction in the maximum dose to the brainstem is associated with a lower risk of radiation-induced injury.

“Gantry w/o LET” and “Gantry with LET opt 1–2” strategies show robustness values that are most comparable to the clinical plan. This is not a negative result; on the contrary, such values indicate that, under the given constraints, the dose distribution remains reliable and well-controlled.

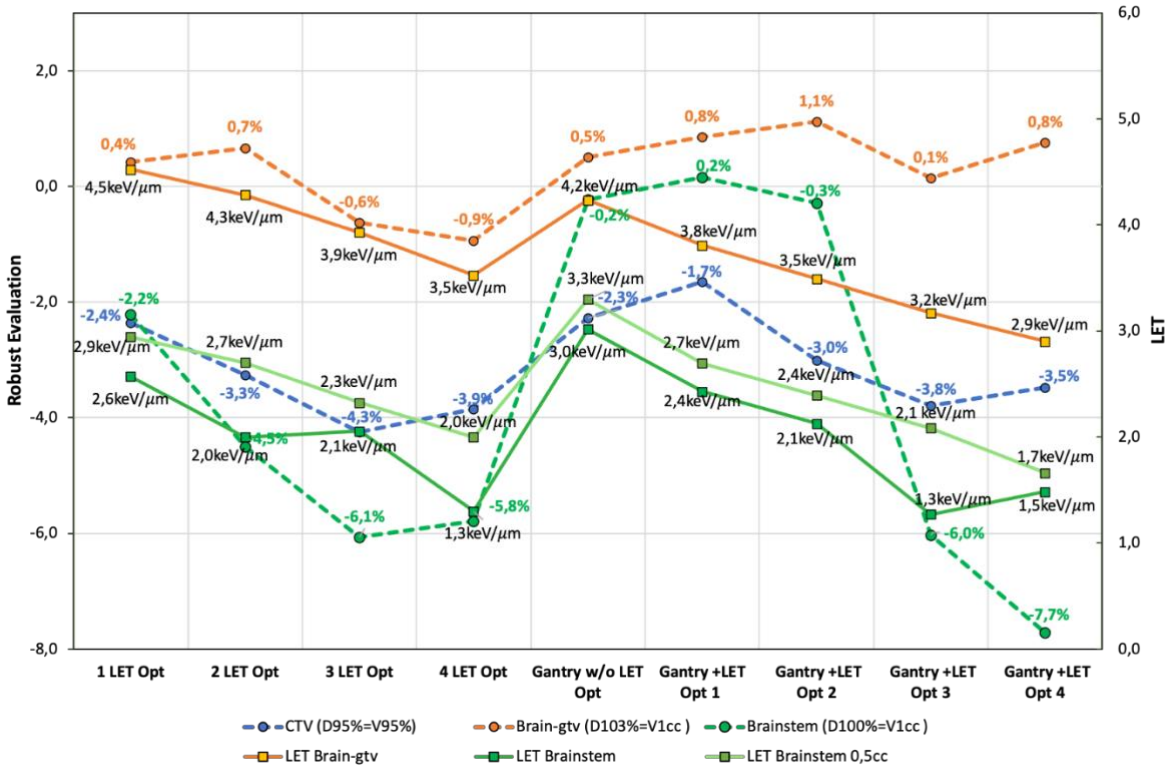

Figure 33. *Relationship Between LETd Values and Robustness for Various Optimization Strategies*

Figure 33 presents a comprehensive overview of the relationship between LETd values and robustness metrics for both critical structures (brain and brainstem), as well as for the CTV. Overall, it can be observed that the approaches “LET opt 1” and “Gantry w/o LET” achieve a

reduction in LET to clinically acceptable levels. Specifically, the LETd value for the brainstem in the first case is 2.6 keV/µm, and slightly higher in the second—3.0 keV/µm. For the brain, the LETd value is lower than 4.6 keV/µm in both cases (4.5 and 4.2 keV/µm), which is clinically acceptable for both. Meanwhile, the reduction in CTV coverage compared to the clinical plan remains within 1% (with a maximum robustness deviation of up to 2.4%), as reported in ***Table 4***. This indicates that even with moderate LET constraints, it is possible to reach borderline LETd values without significantly compromising target coverage or overall plan quality. Furthermore, a reduction in LET can be achieved simply by changing the beam geometry (i.e., transition to gantry-based delivery), even without LET optimization.

The "LET opt 2–3" approaches allow for a more substantial reduction in LETd values, while tolerating a slight decrease in CTV coverage—up to 2.2% relative to the clinical plan (robustness deviation up to 4.3%, which remains clinically acceptable), as reported in ***Table 4***. At the same time, there is a notable reduction in the maximum brainstem dose under the worst-case scenario—by as much as 8.7%, which is a favorable outcome. However, the robustness for the brainstem under these settings drops to 6.1%, indicating reduced stability of the dose distribution.

The "Gantry with LET opt 1–2" strategies also provide considerable LET reduction, while achieving a better balance between optimization and plan quality. Compared to "LET opt 2–3," the CTV coverage loss is halved—up to 1.1% (robustness up to 3%). Additionally, the brainstem's maximum dose in the worst-case scenario shows high robustness (±0.3%), making this approach more balanced.

The most significant LET reduction is achieved with the "Gantry with LET opt 3–4" strategies: LETd values for the brain decrease from 5.1 to 2.9 keV/µm, and for the brainstem from 3.9 to 1.7 keV/µm. In this case, the loss in CTV coverage reaches up to 2.1% (robustness up to 3.8%), and the maximum dose to the brainstem is reduced by 11.1%. However, the dose robustness in the brainstem drops to 7.7%, which exceeds the clinically acceptable threshold.

A comparison of LETd values within the clinical target volume (CTV) was also conducted, given that LET in this region directly influences the potential biological effectiveness of proton radiation. ***Figure 34*** presents the results, demonstrating that LETd values within the CTV

remained largely unchanged following the application of various LET optimization strategies. The stability of LET in the CTV confirms that optimizing LET distribution in healthy tissues does not adversely affect the LET profile within the target.

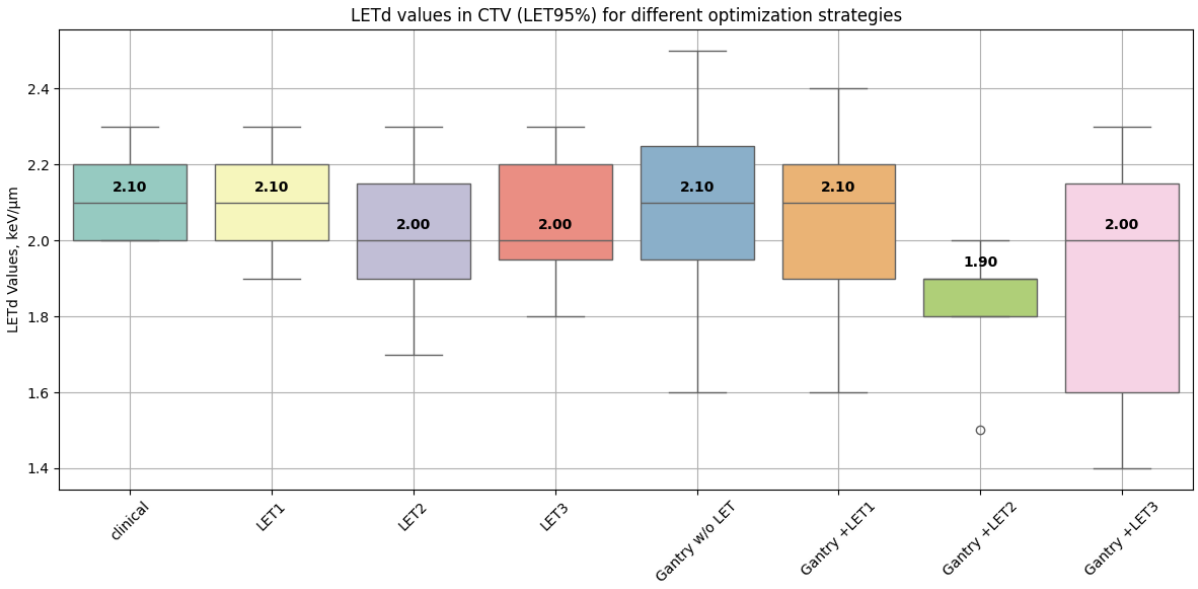

Figure 34. *LETd values at 95% of the prescription dose in the CTV (LET95%) for different optimization strategies*

To compare the outcomes of the LET-optimized approaches with the NTCP curve derived from clinical data, the volume of brain tissue receiving doses above 43 GyE was analyzed for all evaluated plans. These values are presented in ***Figure 35***. As shown in the graph, the brain volume exposed to high doses gradually decreases as the LET constraints become stricter, revealing a monotonic trend between the volume of brain tissue receiving doses above 43 GyE and the LETd optimization strategies adopted, comprising fixed and gantry beam geometry.

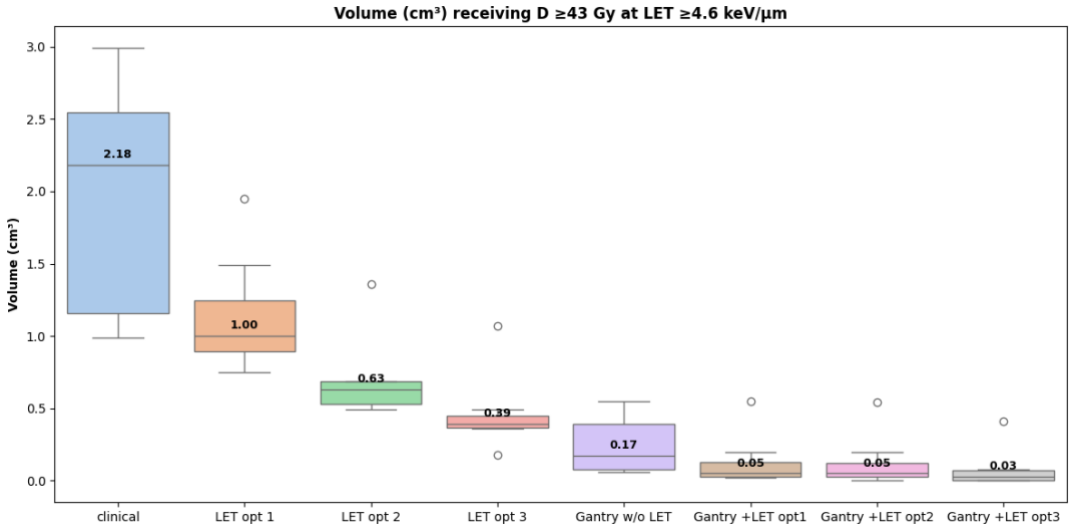

Figure 35. *Volume of brain tissue (cc) receiving a dose above 43 GyE for all optimization approaches and for the clinical plan*

In a prospective scenario, an optimal threshold value is now available in the clinical setting: the volume of brain tissue (cc) receiving more than 43 GyE. It should be noted, however, that pushing the optimization below this threshold might compromise the dose distribution in terms of both quality and robustness. This trade-off is illustrated in ***Figures 36*** and ***37***, which show the reduction in target coverage under the worst-case scenario (CTV D95% compared to the clinical plan), and the variation in the Homogeneity Index (*HI*) as a function of brain volumes receiving more than 43 GyE. These values are reported for all LETd-optimized approaches, separately for fixed beam and gantry delivery techniques.

For a fixed beam geometry, this value could be identified between 0.39 cc and 1 cc, while the additional degrees of freedom available in a gantry geometry allowed to lower this value around 0.3 cc.

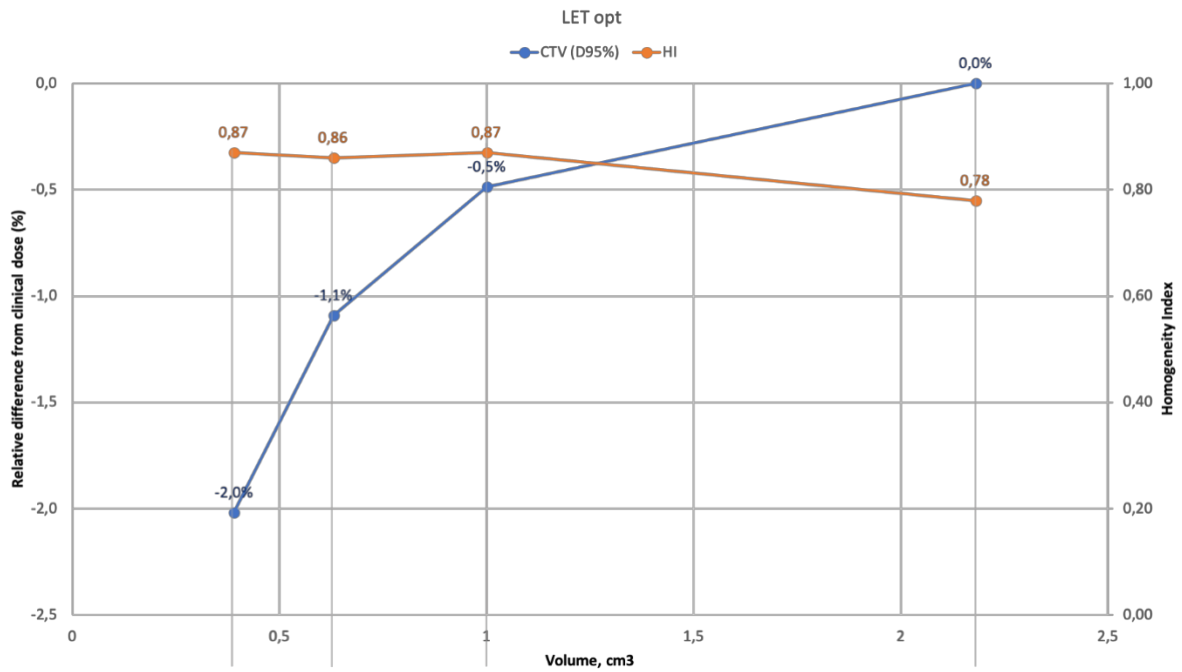

Figure 36. *Relative reduction in CTV D95% (blue line) and the Homogeneity Index (HI, orange line), as a function of and brain volume (cc) receiving >43 GyE, which showed a monotonic relation with the different LET optimization strategies without gantry-geometry (see* ***Figure 35****)*

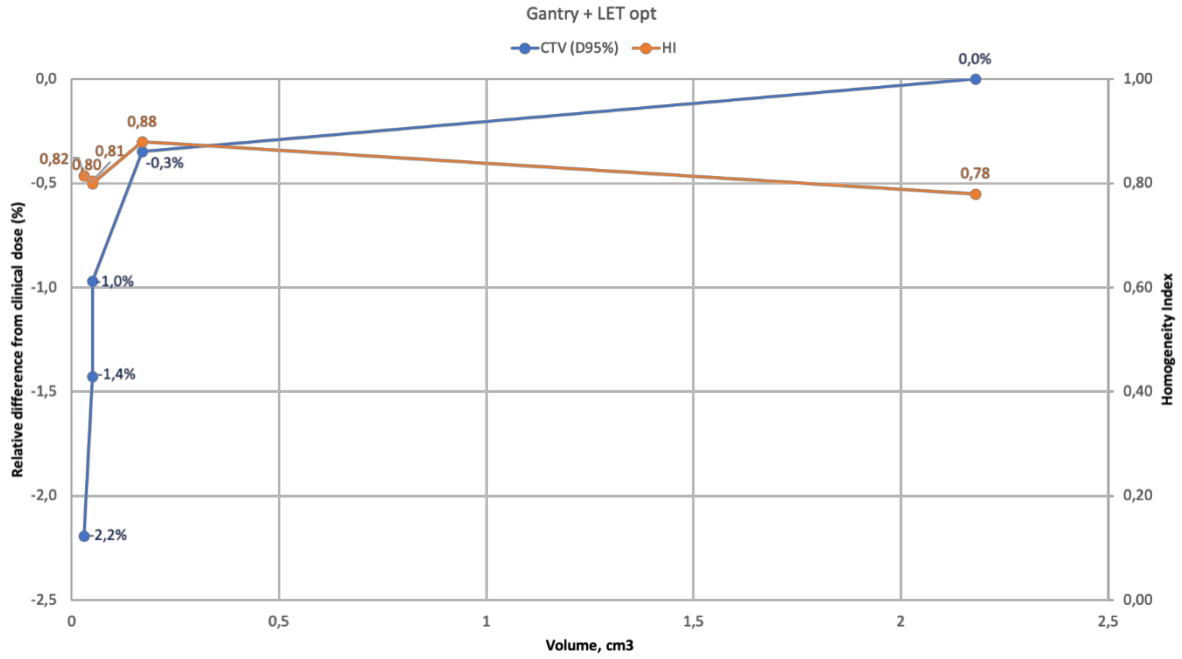

Figure 37. *Relative reduction in CTV D95% (blue line) and the Homogeneity Index (HI, orange line), as a function of and brain volume (cc) receiving >43 GyE, which showed a monotonic relation with the different LET optimization strategies with gantry-geometry*

Applying this approach to the curve of secondary adverse effects as a function of LET, we mapped the values of NTCP as a function of brain volumes receiving more than 43 GyE, focusing on the range of small volumes of particular clinical interest (***Figure 38***).

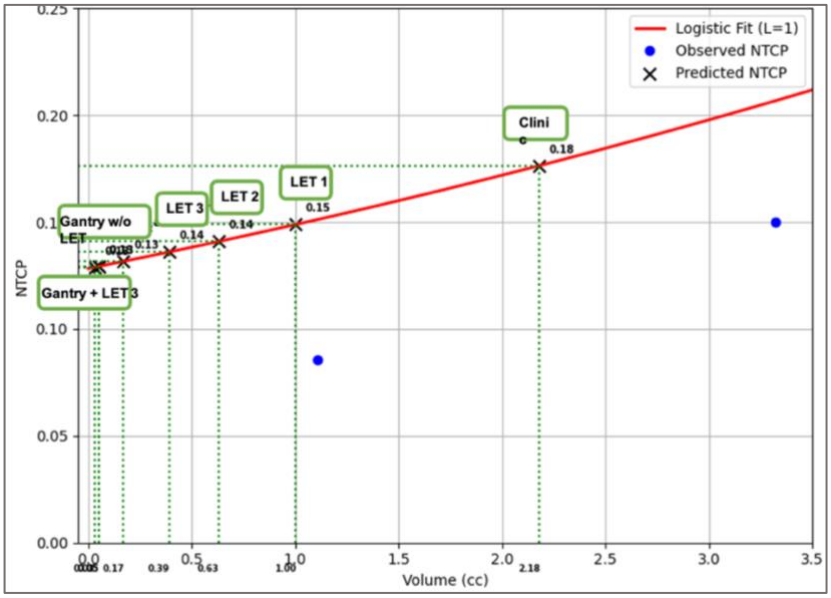

Figure 38. *Positioning of optimization strategies on the enlarged segment of the NTCP curve, focusing on small brain volumes receiving doses above 43 GyE*

NTCP values are a standard method in radiotherapy to assess a priori the best treatment option between two or more competing modalities in terms of expected treatment-induced side effects, with a reduction of approximately 5% and 10% for G2 and G3 toxicities, respectively, considered significant [38]. With reference to ***Figure 39***, where the NTCP values are reported as a function of different LETd optimization strategies, we arbitrarily selected a 3%–5% difference in the expected probability of secondary effects as a threshold to define which optimization modality is preferable compared to the clinical plan. Specifically, the NTCP decreased by 4% for the "LET opt 3" approach and by 5.6% for the "Gantry + LET opt 3" strategy. For this comparison, data from 7 patients were used, as only these cases underwent optimization up to both the "LET opt 3" and "Gantry + LET opt 3" stages. Further optimization was performed only if CTV coverage remained ≥95% of the prescribed dose. This preliminary finding needs to be confirmed by analyzing a larger patient cohort.

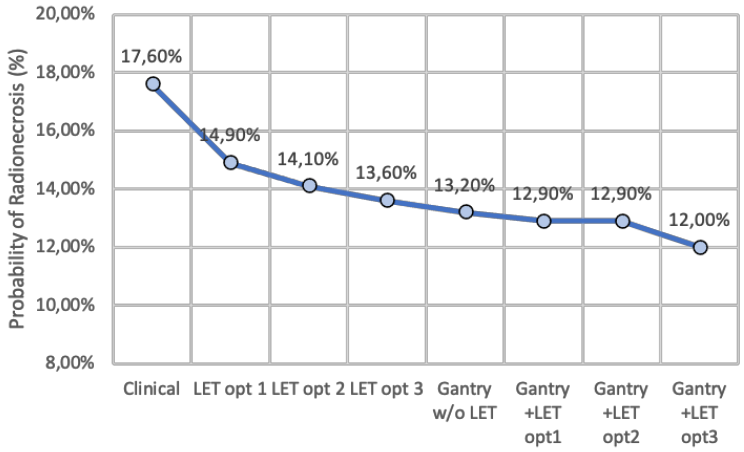

***Figure 39**. Probability of brain necrosis (NTCP) for all planning approaches and the clinical plan, calculated using the predictive model*

This study presents several notable strengths. First, a wide range of optimization strategies—both fixed-beam and gantry-based—were systematically evaluated, allowing for a comprehensive comparison of their dosimetric and clinical impact. Second, the proposed approaches were tested on real clinical plans developed in a state-of-the-art treatment planning system currently used in clinical practice, ensuring the practical relevance and applicability of the findings.

Furthermore, the study incorporated multiple layers of analysis, including plan quality metrics (conformity, homogeneity, and robustness), LETd distributions in both target and organs at risk, and NTCP modeling. Importantly, the results were interpreted not only from a physical dosimetric perspective but also in terms of their clinical significance, by correlating with established thresholds for brain necrosis derived from retrospective patient data. This integration of clinical and dosimetric perspectives reinforces the robustness and translational value of the study.

However, the study also has limitations. The primary limitation is the relatively small patient cohort (n=20), which may constrain the statistical generalizability of the findings. Additionally, for some specific comparisons (e.g., NTCP reduction in later optimization stages), only a subset of patients (n=7) was available, as further optimization was only feasible when CTV coverage remained above the clinical threshold. Despite this, the consistency observed across multiple analytical dimensions strengthens the confidence in the conclusions drawn.

Conclusion

This master's thesis has demonstrated that it is possible to effectively reduce LETd values in healthy brain structures—specifically the brain and brainstem—through various optimization strategies, while maintaining clinically acceptable plan quality in terms of target coverage and robustness.

The retrospective and dosimetric analyses demonstrated that LETd-optimized plans may reduce the risk of radiation-induced toxicity by 2.7–5.6%, as evidenced by a corresponding decrease in NTCP values. Notably, gantry-based plans combined with LET constraints (e.g., "Gantry with LET opt 3") offered the greatest reduction in LETd within critical structures, while preserving dose conformity and homogeneity within the target volume.

Additionally, the analysis confirmed that LETd reduction in healthy tissue does not negatively affect the LETd profile within the target (CTV), thereby supporting the biological effectiveness of the treatment. Importantly, all strategies that maintained CTV coverage above 95% and robustness within ±5% were considered clinically acceptable.

The NTCP modeling validated the clinical relevance of LETd-based constraints by showing that even moderate reductions in LETd-exposed volumes corresponded to meaningful reductions in predicted complication probabilities.

Ultimately, this work highlights that incorporating LETd constraints into plan optimization—especially in combination with flexible beam geometries—can enhance treatment safety without compromising effectiveness. The proposed strategies may serve as practical and clinically relevant guidelines for LETd proton therapy planning for brain tumors.

References

[1] U. Gaikwad, J. Bajpai, and R. Jalali, "Combinatorial approach of immuno-proton therapy in cancer: rationale and potential impact," *Asia Pac J Clin Oncol*, vol. 20, no. 2, pp. 188–197, 2024.

[2] I. Alessi *et al.*, "Short and long-term toxicity in pediatric cancer treatment: central nervous system damage," *Cancers (Basel)*, vol. 14, no. 6, p. 1540, 2022.

[3] H. Paganetti, "Relative biological effectiveness (RBE) values for proton beam therapy. Variations as a function of biological endpoint, dose, and linear energy transfer," *Phys Med Biol*, vol. 59, no. 22, p. R419, 2014.

[4] M. Durante and J. S. Loeffler, "Charged particles in radiation oncology," *Nat Rev Clin Oncol*, vol. 7, no. 1, pp. 37–43, 2010.

[5] R. Mohan and D. Grosshans, "Proton therapy–present and future," *Adv Drug Deliv Rev*, vol. 109, pp. 26–44, 2017.

[6] W. D. Newhauser and R. Zhang, "The physics of proton therapy," *Phys Med Biol*, vol. 60, no. 8, p. R155, 2015.

[7] E. T. Vitti and J. L. Parsons, "The radiobiological effects of proton beam therapy: impact on DNA damage and repair," *Cancers (Basel)*, vol. 11, no. 7, p. 946, 2019.

[8] A. J. Lomax, "Intensity modulated proton therapy and its sensitivity to treatment uncertainties 1: the potential effects of calculational uncertainties," *Phys Med Biol*, vol. 53, no. 4, p. 1027, 2008.

[9] A. Bertolet and A. Carabe, "Proton monoenergetic arc therapy (PMAT) to enhance LETd within the target," *Phys Med Biol*, vol. 65, no. 16, p. 165006, 2020.

[10] W. Gu, R. Neph, D. Ruan, W. Zou, L. Dong, and K. Sheng, "Robust beam orientation optimization for intensity-modulated proton therapy," *Med Phys*, vol. 46, no. 8, pp. 3356–3370, 2019.

[11] A. Fredriksson and R. Bokrantz, "A critical evaluation of worst case optimization methods for robust intensity-modulated proton therapy planning," *Med Phys*, vol. 41, no. 8Part1, p. 081701, 2014.

[12] J. Unkelbach, P. Botas, D. Giantsoudi, B. L. Gorissen, and H. Paganetti, "Reoptimization of intensity modulated proton therapy plans based on linear energy transfer," *Int J Radiat Oncol Biol Phys*, vol. 96, no. 5, pp. 1097–1106, 2016.

[13] D. J. Indelicato *et al.*, "Consensus report from the Stockholm pediatric proton therapy conference," *Int J Radiat Oncol Biol Phys*, vol. 96, no. 2, pp. 387–392, 2016.

[14] J. Sun, "Implementation of 2-step intensity modulated arc therapy," 2010.

[15] S. M. Bentzen *et al.*, "Quantitative Analyses of Normal Tissue Effects in the Clinic (QUANTEC): an introduction to the scientific issues," *Int J Radiat Oncol Biol Phys*, vol. 76, no. 3, pp. S3–S9, 2010.

[16] A. Bolsi, A. Fogliata, and L. Cozzi, "Radiotherapy of small intracranial tumours with different advanced techniques using photon and proton beams: a treatment planning study," *Radiotherapy and oncology*, vol. 68, no. 1, pp. 1–14, 2003.

[17] B. G. Baumert, A. J. Lomax, V. Miltchev, and J. B. Davis, "A comparison of dose distributions of proton and photon beams in stereotactic conformal radiotherapy of brain lesions," *Int J Radiat Oncol Biol Phys*, vol. 49, no. 5, pp. 1439–1449, 2001.

[18] Z. Chen, M. M. Dominello, M. C. Joiner, and J. W. Burmeister, "Proton versus photon radiation therapy: A clinical review," *Front Oncol*, vol. 13, p. 1133909, 2023.

[19] S. Gaito *et al.*, "Normal tissue complication probability modelling for toxicity prediction and patient selection in proton beam therapy to the central nervous system: a literature review," *Clin Oncol*, vol. 34, no. 6, pp. e225–e237, 2022.

[20] E. Bahn, J. Bauer, S. Harrabi, K. Herfarth, J. Debus, and M. Alber, “Late contrast enhancing brain lesions in proton-treated patients with low-grade glioma: clinical evidence for increased periventricular sensitivity and variable RBE,” *Int J Radiat Oncol Biol Phys*, vol. 107, no. 3, pp. 571–578, 2020.
[21] H. Paganetti *et al.*, “Report of the AAPM TG-256 on the relative biological effectiveness of proton beams in radiation therapy,” *Med Phys*, vol. 46, no. 3, pp. e53–e78, 2019.
[22] S. J. McMahon, H. Paganetti, and K. M. Prise, “LET-weighted doses effectively reduce biological variability in proton radiotherapy planning,” *Phys Med Biol*, vol. 63, no. 22, p. 225009, 2018.
[23] C. Hahn *et al.*, “Comparing biological effectiveness guided plan optimization strategies for cranial proton therapy: potential and challenges,” *Radiation Oncology*, vol. 17, no. 1, p. 169, 2022.
[24] I. C. on R. U. and Measurements, *ICRU Report 83 Prescribing, Recording, and Reporting Photon-beam Intensity-modulated Radiation Therapy (IMRT)-Journal of the ICRU-Vol 10 No 1 2010*. Oxford University Press, 2010.
[25] M. Schlachter, R. G. Raidou, L. P. Muren, B. Preim, P. M. Putora, and K. Bühler, “State-of-the-Art Report: Visual Computing in Radiation Therapy Planning,” *Computer Graphics Forum*, vol. 38, no. 3, pp. 753–779, Jun. 2019, doi: https://doi.org/10.1111/cgf.13726.
[26] M. Stock *et al.*, “Harmonization of proton treatment planning for head and neck cancer using pencil beam scanning: first report of the IPACS collaboration group,” *Acta Oncol (Madr)*, vol. 58, no. 12, pp. 1720–1730, 2019.
[27] A. J. Lomax, “Intensity modulated proton therapy and its sensitivity to treatment uncertainties 1: the potential effects of calculational uncertainties,” *Phys Med Biol*, vol. 53, no. 4, p. 1027, 2008.
[28] A. J. Lomax, “Intensity modulated proton therapy and its sensitivity to treatment uncertainties 2: the potential effects of inter-fraction and inter-field motions,” *Phys Med Biol*, vol. 53, no. 4, p. 1043, 2008.
[29] B. Schaffner and E. Pedroni, “The precision of proton range calculations in proton radiotherapy treatment planning: experimental verification of the relation between CT-HU and proton stopping power,” *Phys Med Biol*, vol. 43, no. 6, p. 1579, 1998.
[30] J. Unkelbach, T. Bortfeld, B. C. Martin, and M. Soukup, “Reducing the sensitivity of IMPT treatment plans to setup errors and range uncertainties via probabilistic treatment planning,” *Med Phys*, vol. 36, no. 1, pp. 149–163, 2009.
[31] D. Pflugfelder, J. J. Wilkens, and U. Oelfke, “Worst case optimization: a method to account for uncertainties in the optimization of intensity modulated proton therapy,” *Phys Med Biol*, vol. 53, no. 6, p. 1689, 2008.
[32] J. Unkelbach, T. C. Y. Chan, and T. Bortfeld, “Accounting for range uncertainties in the optimization of intensity modulated proton therapy,” *Phys Med Biol*, vol. 52, no. 10, p. 2755, 2007.
[33] A. Fredriksson, L. Glimelius, and R. Bokrantz, “The LET trilemma: conflicts between robust target coverage, uniform dose, and dose-averaged LET in carbon therapy,” *Med Phys*, vol. 50, no. 12, pp. 7338–7348, 2023.
[34] A. Bazani *et al.*, “2693 Investigation of the combined effect of dose and linear energy transfer on brain necrosis after proton therapy,” *Radiotherapy and Oncology*, vol. 206, pp. S3508–S3509, 2025.
[35] P. Lægdsmand *et al.*, “Variations in linear energy transfer distributions within a European proton therapy planning comparison of paediatric posterior fossa tumours,” *Phys Imaging Radiat Oncol*, vol. 32, p. 100675, 2024.

[36] A. H. Handeland *et al.*, “Linear energy transfer-inclusive models of brainstem necrosis following proton therapy of paediatric ependymoma,” *Phys Imaging Radiat Oncol*, vol. 27, Jul. 2023, doi: 10.1016/j.phro.2023.100466.
[37] L. F. Fjæra *et al.*, “A case-control study of linear energy transfer and relative biological effectiveness related to symptomatic brainstem toxicity following pediatric proton therapy,” *Radiotherapy and Oncology*, vol. 175, pp. 47–55, Oct. 2022, doi: 10.1016/j.radonc.2022.07.022.
[38] G. Fontana *et al.*, “Envisioning an Italian Head and Neck Proton Therapy Model-Based Selection: Challenge and Opportunity,” *Int J Part Ther*, vol. 16, p. 100745, 2025, doi: https://doi.org/10.1016/j.ijpt.2025.100745.

Patients	1 LET Optimization for both structures. Brainstem 2,5 keV/µm, 50Gy, 5%; Brain-gtv 4,6 keV/µm, 43Gy, 0,3%					2 LET Optimization for both structures. Brainstem 2 keV/µm, 50Gy, 3,5%; Brain-gtv 4,2 keV/µm, 43Gy, 0,3%					3 LET Optimization for both structures. Brainstem 1,5 keV/µm, 50Gy, 2%; Brain-gtv 3,8 keV/µm, 43Gy, 0,3%					4 LET Optimization for both structures. Brainstem 1 keV/µm, 50Gy, 1%; Brain-gtv 3,4 keV/µm, 43Gy, 0,3%				
	CTV (D95%)	% from $D_{presc.}$	LET Brain (50Gy, 1cc)	LET Brainstem (50Gy,1cc)	LET Brainstem (50Gy,0,5cc)	CTV (D95%)	% from $D_{presc.}$	LET Brain (50Gy, 1cc)	LET Brainstem (50Gy,1cc)	LET Brainstem (50Gy,0,5cc)	CTV (D95%)	% from D_{presc}	LET Brain (50Gy, 1cc)	LET Brainstem (50Gy,1cc)	LET Brainstem (50Gy,0,5cc)	CTV (D95%)	% from D_{presc}	LET Brain (50Gy, 1cc)	LET Brainstem (50Gy,1cc)	LET Brainstem (50Gy,0,5cc)
BLO_7	53,83	96,5	4,5	2,6	2,75	53,77	96,4	4,15	2,55	2,85	53,55	96	3,85	2,55	2,8	53,29	95,5	3,55	2,75	3,05
BLO_14	53,18	95,3	4,6	2,7	2,85															
BLO_23	53,15	95,3	4,6	2,9	3,25															
BLO_25	53,96	96,7	4,6	2,3	2,55	53,47	95,8	4,3	1,85	2,35										
BLO_26	53,35	95,6	4,2	2,6	2,75															
BLO_31	53,79	96,4	4,3	0	3,05	53,57	96	4,15	0	2,95	53,05	95,1	3,75	0	2,75					
BLO_32	53,96	96,7	4,45	2,45	3,05	53,97	96,7	4,85	2,05	3,35	53,27	95,5	4,75	0	2,25					
BLO_36	53,86	96,5	4,6	2,65	3,55	53,71	96,3	4,25	2,55	3,35	53,24	95,4	3,8	0	2,65					
BLO_37	53,16	95,3	4,45	2,45	2,55															
BLO_38	54,53	97,7	4,6	3,05	4,75	53,47	95,8	4,25	3,85	4,95										
BLO_39	53,31	95,5	4,35	2,35	2,75															
BLO_5	53,08	95,1	4,65	2,65	2,85															
BLO_6	54,31	97,3	4,65	2,5	2,8	54,22	97,2	4,25	2,65	2,85	54,01	96,8	3,85	2,25	2,8	53,48	95,8	3,45	2,45	2,75
BLO_19	53,98	96,7	4,55	2,4	2,5	53,54	95,9	4,2	2,1	2,2	53,17	95,3	3,85	2	2,05					
BLO_22	53,11	95,2	4,65	2,85	3,25															
BLO_40	54,7	98	4,45	2,5	3,25	54,39	97,5	4,15	2,05	2,75	53,3	95,5	3,75	2,25	2,75					
BLO_41	52,96	94,9	4,5	2,25	2,5															
BLO_42	54,19	97,1	4,75	0	2,3	54,2	97,1	4,45	0	0	54,13	97	4,05	0	0	53,85	96,5	3,75	0	0
BLO_43	54,14	97	4,65	2,5	2,85	54,03	96,8	4,25	1,95	2,55	52,94	94,9	3,9	1,75	2,65					
BLO_1	54,4	97,5	4,35	2,55	2,75	54,59	97,8	4,15	2,05	2,55	54,08	96,9	3,75	2,1	2,55	53,25	95,4	3,35	0	2,2
Average	***53,7***	***96,3***	***4,5***	***2,3***	***2,9***	***53,9***	***96,6***	***4,3***	***2***	***2,7***	***53,5***	***95,8***	***3,9***	***1,3***	***2,3***	***53,5***	***95,8***	***3,5***	***1,3***	***2***
Median	53,8	96,5	4,6	2,5	2,8	53,9	96,5	4,3	2,1	2,8	53,3	95,5	3,9	1,9	2,7	53,4	95,7	3,5	1,2	2,5
IQR	1	1,8	0,2	0,3	0,4	0,6	1,2	0,1	0,6	0,6	0,7	1,3	0,1	2,2	0,4	0,3	0,6	0,2	2,5	1,2
Stand. Dev.	0,5	1,0	0,1	0,8	0,5	0,4	0,7	0,2	1,1	1,1	0,4	0,8	0,3	1,1	0,9	0,3	0,5	0,2	1,5	1,4

Appendix Table 1. *Dose coverage and LETd values during the iterative LETd re-optimization process.*
Plans that initially maintained acceptable target coverage — defined as above 96% of the prescribed dose — were further re-optimized with stricter LET constraints for both brain and brainstem until coverage dropped below the clinically acceptable threshold of 95%.

	Gantry with LET Opt 1					Gantry with LET Opt 2					Gantry with LET Opt 3					Gantry with LET Opt 4				
	CTV (D95%)	% from Dpresc.	LET Brain (50Gy, 1cc)	LET Brainstem (50Gy,1cc)	LET Brainstem (50Gy,0,5cc)	CTV (D95%)	% from Dpresc.	LET Brain (50Gy, 1cc)	LET Brainstem (50Gy,1cc)	LET Brainstem (50Gy,0,5cc)	CTV (D95%)	% from Dpresc.	LET Brain (50Gy, 1cc)	LET Brainstem (50Gy,1cc)	LET Brainstem (50Gy,0,5cc)	CTV (D95%)	% from Dpresc.	LET Brain (50Gy, 1cc)	LET Brainstem (50Gy,1cc)	LET Brainstem (50Gy,0,5cc)
Patients	Brainstem 2,5 keV/µm, 50Gy, 5% Brain-gtv 3,8 keV/µm, 43Gy, 0,3%					Brainstem 2 keV/µm, 50Gy, 3,5% Brain-gtv 3,4 keV/µm, 43Gy, 0,3%					Brainstem 1,5 keV/µm, 50Gy, 2% Brain-gtv 3 keV/µm, 43Gy, 0,3%					Brainstem 1 keV/µm, 50Gy, 1% Brain-gtv 2,6 keV/µm, 43Gy, 0,3%				
BLO_7	53,66	96,2	4	3,2	3,35	53,44	95,8	3,65	3,15	3,25										
BLO_14	53,01	95,0	3,8	2,5	2,85															
BLO_23	54,19	97,1	3,95	2,45	3,15	53,38	95,7	3,55	2,1	2,75										
BLO_25	53,79	96,4	3,95	2,95	3,35	53,59	96,0	3,65	2,85	3,3	53,1	95,2	3,45	2,55	3,1					
BLO_26	53,49	95,9	3,8	2,4	2,5															
BLO_31	55,47	99,4	3,65	2,35	2,45	55,42	99,3	3,4	1,85	1,95	53,84	96,5	3,05	0	2,05	53,2	95,3	2,75	0	1,8
BLO_32	54,17	97,1	4,05	2,1	2,25	54,13	97,0	3,95	1,9	2	53,64	96,1	3,75	2,1	2,4	53,42	95,7	3,65	0	1,55
BLO_36	54	96,8	3,85	2,4	2,5	54,04	96,8	3,5	1,9	2,05	53,54	95,9	3,15	0	2,2					
BLO_37	53,62	96,1	3,8	2,45	2,6	53,04	95,1	3,45	1,95	2,35										
BLO_38	54,97	98,5	3,75	2,3	2,45	54,55	97,8	3,35	1,8	1,95	52,9	94,8	2,95	0	1,95					
BLO_39	54,84	98,3	3,45	2,45	2,65	52,99	95,0	3,25	2,05	2,25										
BLO_5	53,43	95,8	3,85	2,35	2,5															
BLO_6	54,59	97,8	3,85	2,5	2,6	54,17	97,1	3,45	2,35	2,6	53,74	96,3	3,05	2,6	2,75	53,16	95,3	2,7	2,35	2,65
BLO_19	54,01	96,8	3,9	2,3	2,45	53,79	96,4	3,55	1,85	1,95	53,33	95,6	3,15	1,45	1,55					
BLO_22	53,38	95,7	3,85	2,5	3,05															
BLO_40	54,33	97,4	3,55	2,4	2,75	53,21	95,4	3,35	2,45	2,95										
BLO_41	54,58	97,8	3,85	2,45	2,6	54,3	97,3	3,45	2,05	2,35	53,55	96,0	2,95	2,15	2,4	53,08	95,1	2,7	2,1	2,3
BLO_42	53,98	96,7	3,65	2,15	2,35	53,96	96,7	3,5	1,75	1,95	53,92	96,6	3,15	0	0	53,65	96,1	2,7	0	0
BLO_43	53,11	95,2	3,95	1,95	2,95															
BLO_1	53,79	96,4	3,65	2,4	2,55	53,61	96,1	3,35	1,9	2,25	53,01	95,0	3,05	1,85	2,45					
Average	*54,0*	*96,8*	*3,8*	*2,4*	*2,7*	*53,8*	*96,5*	*3,5*	*2,1*	*2,4*	*53,5*	*95,8*	*3,2*	*1,3*	*2,1*	*53,3*	*95,5*	*2,9*	*0,9*	*1,7*
Median	54,0	96,8	3,9	2,4	2,6	53,8	96,4	3,5	2,0	2,3	53,5	96,0	3,1	1,7	2,3	53,2	95,3	2,7	0,0	1,8
IQR	0,8	1,4	0,2	0,1	0,4	0,7	1,3	0,2	0,4	0,7	0,6	1,0	0,1	2,1	0,5	0,3	0,5	0,0	2,1	0,8
Stand. Dev.	0,6	1,1	0,2	0,3	0,3	0,6	1,1	0,2	0,4	0,5	0,4	0,6	0,2	1,1	0,8	0,2	0,4	0,4	1,2	1,0

Appendix Table 2. *Dose coverage and LETd values during the iterative LETd re-optimization process with gantry geometry.*
Plans that initially maintained acceptable target coverage — defined as above 96% of the prescribed dose — were further re-optimized with stricter LET constraints for both brain and brainstem until coverage dropped below the clinically acceptable threshold of 95%.